

Received Date: 06-Nov-2012

Revised Date: 02-Sep-2013

Accepted Date: 12-Nov-2013

Article Type: Original Manuscript

The spatial and temporal distribution of grain-size breaks in turbidites

Stevenson, C.J.¹, Talling, P.J.¹, Masson, D.G.¹, Sumner, E.J.², Frenz, M.³, Wynn, R.B.¹

¹National Oceanography Centre, Southampton,
European Way, Southampton, SO14 3ZH, UK.

²School of Earth and Environment, University of Leeds, Leeds, LS2 9JT, UK

³Micrometrics GmbH, Rutherford 108, 52072 Aachen, Germany

Corresponding author: chris.stevenson@noc.soton.ac.uk

Associate Editor – Jaco Baas

Short Title – Grain-size breaks in turbidites

ABSTRACT

Grain-size breaks are surfaces where abrupt changes in grain size occur vertically within deposits. Grain-size breaks are common features in turbidites around the world, including ancient and modern systems. Despite their widespread occurrence grain-size breaks have been regarded as exceptional, and not included within idealized models of turbidity current deposition. This study uses *ca* 100 shallow sediment cores, from the Moroccan Turbidite System, to map out five turbidite beds for distances in excess of 2000 km. The vertical and spatial distributions of grain-size breaks within these beds are examined. Five different types of grain-size break are found: *Type I* – in proximal areas between coarse sand and finer grained structureless sand; *Type II* – in proximal areas between inversely-graded sand overlain by finer sand; *Type III* – in proximal areas between sand overlain by ripple cross-laminated finer sand; *Type IV* – throughout the system between clean sand and mud; and *Type V* – in distal areas between mud-rich (debrite) sand and mud. This article interprets

This is an Accepted Article that has been peer-reviewed and approved for publication in the *Sedimentology*, but has yet to undergo copy-editing and proof correction. Please cite this article as an “Accepted Article”; doi: 10.1111/sed.12091
This article is protected by copyright. All rights reserved.

Types I and V as being generated by sharp vertical concentration boundaries, controlled by sediment and clay concentrations within the flows, whilst *Types II and III* are interpreted to be products of spatial/temporal fluctuations in flow capacity. *Type IV* are interpreted to be the product of fluid mud layers, which hinder the settling of non-cohesive grains and bypasses them down slope. Decelerating suspensions with sufficient clay will always form cohesive layers near to bed: promoting the generation of *Type IV grain-size breaks*. This may explain why *Type IV grain-size breaks* are widespread in all five turbidites examined and are commonplace within turbidite sequences studied elsewhere. Therefore, *Type IV grain-size breaks* should be understood as the norm, not the exception, and regarded as a typical feature within turbidite beds.

INTRODUCTION

Grain-size breaks are an abrupt change in grain size across an intra-bed surface. Grain-size breaks are a common phenomenon, documented in numerous turbidite systems from around the world (Kuenen, 1953; Ksiazkiewicz, 1954; Birkenmajer, 1958; Bouma, 1962; Walker, 1967; Piper, 1972; Piper 1978; Stanley, 1982; Mutti, 1992; Lebreiro et al., 1997; Gladstone and Sparks, 2002; Kneller and McCaffrey, 2003; Sinclair and Cowie, 2003; Sylvester and Lowe, 2004; Kane et al., 2007; Eggenhuisen et al., 2011; Sumner et al., 2012; Talling et al., 2012a) and also occur within terrestrial gravity current deposits such as pyroclastic flow deposits and ignimbrites (Gladstone and Sparks, 2002; Brown and Branney, 2004; Edmonds and Herd, 2005; Edmonds et al., 2006). Classic turbidite models predict sedimentation from a waning flow to produce a deposit that progressively fines upward (Bouma, 1962; Stow and Bowen, 1978; Stow and Shanmugam, 1980; Lowe, 1982; Stow and Piper, 1984). Although Bouma recognized grain-size breaks as a common feature within turbidites across the Peira-Cava area (Bouma, 1962), they are not included in the Bouma sequence or other idealized facies schemes and represent a significant departure from these widely used models.

Previous work has offered a variety of explanations for the generation of grain-size breaks. First, grain-size breaks can result from major rheological differences between slumps and genetically linked turbidity currents. Such grain-size breaks have been recorded between welded slump/turbidite couplets in proximal slope valley environments (Wood and Smith, 1958; Stanley, 1982). Second, grain-size breaks may result from sharp internal discontinuities in concentration and grain size within the flow. Different types of discontinuity have been

proposed that separate turbidity current and debris flow, particularly within flows transitional between the two (Haughton et al., 2003; Talling et al., 2004; Manica 2012), or the body of a turbidity current from its overlying wake (Książkiewicz, 1954; Gladstone and Sparks, 2002). Third, grain-size breaks can result from flow reflection (Pickering and Hiscott, 1985). Fourth, grain-size breaks can result from flow separation due to topography, whereby the coarser-grained basal part of the flow is diverted to take a different path to the upper finer-grained part of the flow. For example, flows experiencing intra-slope confinement (Sinclair and Cowie, 2003) or complex intra-channel topography (Kane and Hodgson, 2011). Fifth, grain-size breaks result from bypass of intermediate grain sizes for a period of time due to fluctuations in the sediment carrying capacity of the flow (Kneller and McCaffrey, 2003). Sixth, grain-size breaks result from a strongly bimodal initial grain-size distribution within the flow (Bouma, 1962; Kneller and McCaffrey, 2003). A seventh mechanism is proposed here whereby grain-size breaks, from sand to mud, are related to the development of cohesive mud layers towards the rear of the flow (Piper, 1972, 1978; McCave and Jones, 1988; Jones et al., 1992), which are able to support non-cohesive grains and bypass large volumes of sediment downslope. These cohesive mud layers are interpreted to be similar to fluid mud layers documented in shallow water and estuarine settings (McCave and Jones, 1988; Jones et al., 1992). Fluid mud is a mud (silt and clay) suspension with sufficient concentration (>10 g/l) to gel and achieve yield strength (McAnally, 2007a, b). Fluid muds are highly mobile and include streaming underflows and gravity currents (McAnally, 2007a, b).

Many of the proposed mechanisms for the generation of grain-size breaks are difficult to validate. For example, grain-size breaks are likely to develop beneath a flow with a strongly bimodal grain-size distribution (Bouma, 1962; Kneller and McCaffrey, 2003; Kane et al., 2007). However, in order to validate such a hypothesis, it is necessary to analyse the grain size of the entire deposit in order to establish whether or not the parent flow contained the range of grain sizes missing across the grain-size breaks. This analysis requires detailed mapping of individual turbidite beds over their entire depositional extent, which commonly is not possible.

This contribution presents a detailed analysis of five turbidite beds, correlated across the Moroccan Turbidite System situated offshore north-west Africa. These beds provide a rare opportunity to investigate how and why grain-size breaks form. The deposits are unconsolidated, allowing detailed quantification of their grain-size distribution. Analysis of

deposits on the modern sea floor allows the relations between grain-size breaks and changes in sea floor gradient to be established. The excellent core coverage coupled with a robust individual bed correlation framework enables turbidites to be documented over their entire depositional extent, both in down flow and across flow directions. This is arguably the most detailed and extensive correlative framework for individual flow deposits in any turbidite system. It is also by far the largest collection of published grain size measurements (*ca* 1500 samples) made from individual turbidite beds. The specific aims of this study are to:

1. Document the frequency, magnitude and spatial distribution of grain-size breaks within individual turbidite beds across the Moroccan Turbidite System.
2. Use spatially extensive grain-size analysis across the individual turbidites to estimate the total grain-size distributions within entire beds.
3. Relate the distribution of grain-size breaks to changes in sea floor gradient.
4. Use these five deposits to evaluate and develop mechanisms for the formation of grain-size breaks.

The Moroccan Turbidite System

The Moroccan Turbidite System consists of three interconnected deep-water basins (Wynn et al., 2002): the Seine Abyssal Plain in the north-east, the Agadir Basin situated in the central part of the system, and the Madeira Abyssal Plain in the west (Fig. 1). The Seine Abyssal Plain covers an area *ca* 54,000 km² and occupies water depths of between 4300 m and 4450 m. To the west and to the north, the Seine Abyssal Plain is bounded by a series of volcanic seamounts. To the east, it is bounded against the African continental margin (Davies et al., 1997; Wynn et al., 2002). The basin floor has slopes of between *ca* 0.01° and 0.05° with two broad topographic low points situated in the west and central parts of the basin (Wynn et al., 2012). The southern boundary is defined by a spur projecting south-east to north-west from the continental margin, the Casablanca seamount, and a low relief sill (50 to 100 m high) that separates the Seine Abyssal Plain from the adjacent Agadir Basin. The Agadir Basin covers an area *ca* 35, 000 km² and occupies water depths between 4300 m and 4500 m. The Agadir Basin is bordered to the north and south by the volcanic archipelagos of the Madeira and Canary/Selvage Islands. The basin gently slopes towards the south-west with gradients of between <0.01° and 0.03° (Wynn et al., 2010). To the south-west the Agadir Basin opens out onto the Madeira Continental Rise; this is associated with an increase in

slope from *ca* 0.02 to 0.06 and the initiation of the 700 km long Madeira Channel System, a series of shallow (20 m deep and 5 km wide) distributary channels that connect the Agadir Basin with the Madeira Abyssal Plain to the west (Masson, 1994; Stevenson et al., 2012). The Madeira Abyssal Plain is an elongate strip of sea floor trending NNE, which covers an area *ca* 80,000 km² and occupies water depths of *ca* 5000 m (Weaver and Kuijpers, 1983). The western side of the basin is bounded by numerous volcanic seamounts whilst its eastern side is open, extending into the Madeira Continental Rise. Sea floor gradients in the basin are around 0.002° (Weaver and Kuijpers, 1983).

Three main types of turbidite are found within the Moroccan Turbidite System: (i) siliciclastic turbidites sourced from the Moroccan Margin, primarily composed of shallow water biogenic material, quartz and glauconite; (ii) carbonate-rich turbidites sourced from local seamount collapses, composed almost exclusively of foraminifera and carbonate-rich ooze; and (iii) volcanoclastic turbidites sourced from the Canary Islands, which are dominated by volcanic glass and mafic lithics (de Lange et al., 1987; Pearce and Jarvis, 1992; Weaver et al., 1992; Pearce and Jarvis, 1995; Wynn et al., 2002; Hunt et al., 2011). The five turbidites examined in this study are siliciclastic beds sourced from the Moroccan Margin. All beds have similar sand fraction mineralogy and have smectite and illite comprising between *ca* 60% and 80% of the clay mineralogy (Pearce and Jarvis, 1992). The main flow pathways of the siliciclastic flows are via the Agadir and El Jadida Canyons, which debouche directly into the Agadir Basin and Seine Abyssal Plain (Fig. 1). The Madeira Abyssal Plain is situated distally within the system, fed by flows with sufficient volume to run-out beyond the Agadir Basin and pass through the Madeira Channel System (Wynn et al., 2002; Wynn et al., 2010; Stevenson et al., 2012).

MATERIALS AND METHODS

Sea floor bathymetry and gradient

Modern sea floor bathymetry is determined using the General Bathymetric Chart of the Oceans (GEBCO). These data provide bathymetry across the entire Moroccan Turbidite System with a pixel size of *ca* 900 m² (horizontal resolution *ca* 5 km). This resolution is sufficient to define large-scale topographic features such as canyons, seamounts and topographic low points. In addition, hull mounted EM12 swath bathymetry is used in conjunction with GEBCO data across the Madeira Channel System (Stevenson et al., 2012), providing a vertical and horizontal resolution of *ca* 0.02 m and *ca* 350 m, respectively. Sea

floor gradients are calculated from GEBCO spot heights, which were then smoothed within a 3 km² grid. There is good agreement between sea floor gradients calculated from GEBCO data and sea floor gradients calculated between core sites using trigonometry.

Cores

This study is based on *ca* 100 shallow piston cores recovered over the last 30 years during a number of research cruises. Core sites are located throughout the Moroccan Turbidite System both in down flow and across flow directions (Fig. 1). All cores were subject to detailed visual logging with particular attention focused on the turbidite beds. Grain size was initially established with a hand lens and comparison with a grain size comparator card.

Grain-size analysis

Quantitative grain-size analyses were carried out using a Malvern Mastersizer 2000 (Malvern Instruments Limited, Malvern, UK) in combination with a Malvern Hydro G accessory unit and a 36-pot Malvern auto-sampler. The instrument uses laser diffraction to calculate grain sizes between 0.02 to 2000 μm . Samples comprised between 0.5 cm³ and 1.5 cm³ of bulk sediment with coarser sediments requiring larger bulk samples. Samples were added to a 0.05% sodium hexametaphosphate solution and shaken for at least 8 hours to ensure dispersion of flocs. For the analyses, a laser target obscuration of 10 to 20% was obtained for each sample. Particle refractive index was set to 1.52 with an absorption value of 0.1, providing average parameters for a mixed mineral assemblage as expected for marine sediments. Three measurements were carried out on each sample for which average particle-size distributions were calculated.

RESULTS

Sediments in cores

Herein the terms ‘clay’, ‘silt’ and ‘sand’ are used to refer to sediments with grain sizes <8 μm , 8 to 63 μm and >63 μm , respectively. The generic term ‘mud’ is used to collectively refer to silt and clay sediments <63 μm .

Cores collected from the Moroccan Turbidite System contain hemipelagic sediment punctuated by turbidite beds. Hemipelagic sediments deposited during interglacial periods are

light greyish or brownish fine-grained carbonate-rich oozes, containing randomly dispersed foraminifera (Weaver and Kuijpers, 1983; Weaver and Rothwell, 1987; Weaver, 1991). In contrast, hemipelagic sediments deposited during glacial periods are reddish-brown clay with few foraminifera (Weaver and Kuijpers, 1983). Turbidites have characteristically sharp bases with gradational bioturbated upper contacts with hemipelagic sediments. Foraminifera are absent from turbidite muds.

Bed Correlation

Over the past 30 years a robust geochemical and chronostratigraphic framework has been established across the Late Quaternary Moroccan Turbidite System, covering stratigraphy over the past 200 ka. This has enabled individual turbidite beds to be correlated, both in down flow and across flow directions (Weaver and Kuijpers, 1983; de Lange et al., 1987; Pearce and Jarvis, 1992; Rothwell et al., 1992; Weaver et al., 1992; Weaver and Thomson, 1993; Weaver, 1994; Pearce and Jarvis, 1995; Davies et al., 1997; Wynn et al., 2002; Talling et al., 2007c; Frenz et al., 2008). Exceptional core coverage has enabled individual turbidite beds to be correlated between basins, producing an inter-connected turbidite stratigraphy that extends across the entire Moroccan Turbidite System (Wynn et al., 2002). This substantial body of work is built upon here by incorporating a suite of *ca* 70 cores into the established turbidite stratigraphy, recovered aboard *RRS Charles Darwin* Cruise CD166 (2004) and *RRS James Cook* Cruise JC27 (2008). The increased core control enables existing bed correlations to be extended from the base of the Moroccan Margin, across the Seine Abyssal Plain, through the Agadir Basin, into the Madeira Channel System and, ultimately, into the Madeira Abyssal Plain (Fig. 2). Turbidites are numbered sequentially down core, using the nomenclature adopted by Wynn et al. (2002) for the Agadir Basin. Prefixes are used to denote in which part of the Moroccan Turbidite System the beds occur: 'S' for Seine Abyssal Plain, 'A' for the Agadir Basin and connecting Madeira Channel System; and 'M' for the Madeira Abyssal Plain. This study focuses on five turbidites: Beds 3, 5, 7, 11 and 12 (Fig. 2).

Beds 5 and 12 are very large-volume events ($>160 \text{ km}^3$) and have impressive run-outs with deposits extending $>2000 \text{ km}$ across the entire system. Bed 7 is also large-volume (*ca* 120 km^3) with deposits extending *ca* 1500 km from the Agadir Basin to the Madeira Abyssal Plain. Beds 3 and 11 are relatively small-volume (*ca* 15 km^3) and are restricted to proximal parts of the system: the Seine Abyssal Plain and north-east parts of the Agadir Basin.

Turbidite facies

Sedimentary textures found within turbidite beds are described within a facies scheme. Many of the facies described in this study are common to deep-water turbidite systems and have been thoroughly described elsewhere (Bouma, 1962; Lowe, 1982; Sumner et al., 2012; Talling et al., 2012a). For clarity, a brief description of each facies is provided below.

Structureless Sand (ST; Bouma T_A)

Structureless sand comprises sand displaying no sedimentary structures with mud contents typically between 5% and 10% (maximum range up to *ca* 15%). This structureless facies is differentiated from ‘mud-rich structureless sand’ by significantly lower mud content.

Mud-Rich Structureless Sand (ST_D)

Distinctive intervals of mud-rich (40 to 50% mud), structureless sand are found within Bed 5 across the Agadir Basin and eastern parts of the Seine Abyssal Plain. This facies directly overlies relatively clean structureless and parallel laminated sands. It is largely ungraded but can have weak normal grading in places (see Talling et al., 2007c, for more detail).

Laminated Sand (PL, RXL, CL; Bouma T_B and T_C)

Planar laminated sand (PL) is found in all of the turbidites examined in this study, occurring towards the base of deposits. Laminae are relatively thin (<2 mm thick) with low mud contents between 5% and 10%. This facies can have a range of grading patterns including: inverse, normal and ungraded. Ripple cross-laminated sand (RXL) occurs towards the upper parts of deposits, or at the base of relatively thin-bedded turbidites. This facies is normally-graded and, on average, has slightly higher mud content (between 5% and 20%) than parallel laminated sands. Contorted lamination (CL) within sand intervals is common through the basin. This facies typically occurs at mid-height in the bed and has similar mud content to ripple-cross laminated sands between 5% and 25%. Contorted intervals can be inverse and/or normal graded.

Turbidite Mud (L, CM and, M; Bouma T_D and T_E)

Volumetrically, turbidite mud is the most abundant type of sediment within the Moroccan Turbidite System. The clay mineralogy within the muds contains *ca* 60 to 70% smectite and illite with a smaller proportion of kaolinite and chlorite between 30% and 40%

(Pearce and Jarvis, 1992). Basal parts of the mud cap are frequently silt-rich (silt/clay ratios of *ca* 2:1) with thin inter-laminated silts and muds (L). This facies normally grades into ungraded, structureless mud (M) with silt/clay ratios of *ca* 1:1. Frequently, the basal parts of the mud cap, and less frequently within the upper parts of the mud cap, have intervals of contorted silty laminae, some with clasts of silt. These intervals can have multiple fining upward sequences.

Typical geometry of turbidite mud

Most turbidite mud, within the five beds examined, occurs as a relatively thin (10 to 20 cm) drape, overlying coarser sand deposits (Fig. 2). These thin muds are usually ungraded and structureless (M). However, large volumes of mud are ponded in topographic low points within the system. Proximally, this occurs within the Seine Abyssal Plain (north-east parts of Fig. 2). Distally, muds are ponded into the central parts of the Madeira Abyssal Plain (south-west parts of Fig. 2). Ponded muds have silt-rich normally-graded bases, and within the Seine Abyssal Plain have contorted silty laminations and clasts.

Grain-size breaks

Grain-size breaks occur within all of the beds examined in this study and are also present in all other turbidites studied from the Moroccan Turbidite System. Locally, five types of grain-size break are recognized (Fig. 3; Table 1): *Type I grain-size breaks* occur between coarse-grained sand overlain by finer grained sand (Fig. 3Ab). These grain-size breaks are found in Beds 5 and 12; Beds 3 and 11 do not contain sufficiently coarse material for this type of grain-size break to form. Within Bed 5 coarse sand-sized sediment overlain by *Type I grain-size breaks* occurs at the base of the bed along most of the length of the Agadir Basin. In Bed 12 very coarse-grained sediment overlain by *Type I grain-size breaks* only occurs in proximal areas of the Agadir Basin. *Type II grain-size breaks* comprise inversely-graded sand overlain by finer grained sand (Fig. 3Bb). This type of grain-size break occurs in Beds 5 and 12 in proximal areas of the Agadir Basin, notably these are both large volume beds (Wynn et al., 2002; Frenz et al., 2008). *Type III grain size breaks* are rare and comprise planar laminated sands overlain by structureless or contorted very-fine sands (Fig. 3Ca). This type of grain-size break is restricted to proximal localities within Bed 11. *Type IV grain-size breaks* comprise clean sand overlain by a relatively thin turbidite mud (Figs 3Ba, Da and Ea); they occur proximally, centrally and relatively distally (where sand deposits are present) within all five beds. Within the five beds examined, 82% of grain-size transitions from sand

into mud were *Type IV grain-size breaks* as opposed to a gradational transition from sand to mud. *Type IV grain-size breaks* can be overlain by a range of turbidite mud facies: (i) mud with a normally-graded base (occasionally with interlaminated silts; Fig. 3Ea); (ii) ungraded structureless mud (Fig. 3Da); or (iii) mud with contorted silty laminations and/or silt clasts (Fig. 3Ba). However, where turbidite muds are ponded, *Type IV grain-size breaks* generally are absent with deposits grading from sand into contorted muds. *Type V grain-size breaks* comprise mud-rich structureless sand overlain by ungraded turbidite mud (Fig. 3Aa). This type of grain-size break only occurs in Bed 5 and is restricted to distal localities.

Grain-size distributions and grain-size breaks within individual beds

Vertical grain-size profiles and spatial distributions of all types of grain-size break are presented, in detail, for Beds 3, 5, 7, 11 and 12. In addition, total grain-size distributions are shown for each bed, which are the sum of all grain-size distributions measured in each basin within each bed (Fig. 4). Total grain-size distributions are considered to be representative of the overall grain-size distribution within each bed because: (i) grain-size measurements were as evenly distributed as possible, vertically within each bed and spatially throughout the system; and (ii) a substantial number of grain-size samples were analyzed (*ca* 1500). Total grain-size distributions for each basin are weighted according to total deposit volume.

Bed 3

Bed 3 is a relatively small-volume turbidite (*ca* 13 km³), which thins and fines rapidly from north-east to south-west along the Agadir Basin, yet extends throughout the Seine Abyssal Plain. Sand deposits are typically thin (<12 cm) and are restricted to proximal areas of the system, particularly around the mouths of the Agadir and El Jadida Canyons. Sand intervals are all normally-graded across the Agadir Basin and Seine Abyssal Plain (Fig. 5A).

Type IV grain-size breaks from sand to ungraded mud primarily occur around the mouth of the Agadir Canyon and across the Safi Plateau (Fig. 5B). Within some areas *Type IV grain-size breaks* are overlain by muds with normally-graded bases. Normally-graded transitions between sand and mud occur close to the margins of the Agadir Basin and Seine Abyssal Plain.

Total grain-size distributions calculated from deposits situated in the Agadir Basin and Seine Abyssal Plain are relatively similar (Fig. 4). Bed 3 has a broadly unimodal grain-size distribution between *ca* 20 μm to *ca* 100 μm . The grain-size distribution of deposits within the Seine Abyssal Plain is coarser, from *ca* 20 μm to *ca* 200 μm .

Bed 5

This large-volume turbidite (>160 km³) is recorded in all three basins. Relatively thick (*ca* 40 to 120 cm), coarse-grained (up to *ca* 1000 µm), structureless and parallel laminated, clean sands occur throughout the Seine Abyssal Plain and across most of the Agadir Basin (Talling et al., 2007c; Frenz et al., 2008; Wynn et al., 2010; Sumner et al., 2012). *Type I and II grain-size breaks* are common in proximal localities, i.e. close to the mouth of the Agadir Canyon, (Fig. 6A) occurring between coarse-grained sand and inversely-graded sands at the base of deposits (*ca* 900 to 1000 µm), overlain by finer ungraded clean sand (*ca* 100 to 200 µm; Fig. 7 Core CD166/57). However, occasional thin deposits of coarse sand are found more distally, overlain by *Type I grain-size breaks*. Sand deposits found across the Madeira Channel System comprise thinner (*ca* 10 to 20 cm), finer (up to *ca* 250 µm) parallel and ripple cross-laminated sands. *Type III grain-size breaks* are occasionally found in this area, occurring between normally-graded ripple cross-laminated sands (*ca* 80 µm) overlain by finer grained parallel laminated sand (*ca* 60 µm; Stevenson et al., 2012). Across the Safi Plateau (south of the Seine Abyssal Plain) *Type III grain-size breaks* are found between very thin (*ca* 5 cm thick) structureless sands overlain by parallel laminated sands (Fig. 6A).

Type IV grain-size breaks are found throughout the deposit (Fig. 6B), occurring between inverse-graded, normal-graded and ungraded clean sands (*ca* 60 to 80 µm) overlain by ungraded, graded and contorted muds (*ca* 15 to 25 µm; Fig. 7 Core D11938). Across the Agadir Basin overlying muds are relatively thin (10 to 20 cm). In contrast, turbidite muds found across the Seine Abyssal Plain are generally thicker (*ca* 10 to 250 cm). A single normally-graded deposit (from sand to mud) is found in the central part of the basin (Fig. 6B), which has thick (*ca* 250 cm) ponded mud cap with contorted laminations and silty clasts. Contorted muds overlying *Type IV grain-size breaks* dominate across the other parts of the Seine Abyssal Plain (Fig. 7, Core D11938). Mud-rich sand deposits found proximal to the mouths of the Agadir and El Jadida Canyons, have normal grading between mud-rich sand and overlying turbidite mud (Fig. 7, Cores CD166/57 and JC27/19). In contrast, every mud-rich sand deposit situated in the relatively distal, south-east part of the Agadir Basin is overlain by a *Type V grain-size break* which is, in turn, overlain by ungraded mud (Fig. 6B; Fig. 7, Core CD166/12).

Deposits within the Madeira Abyssal Plain are mostly fine-grained with silt-rich normally-graded bases overlain by ungraded turbidite mud (Fig. 7, Core D11813) (McCave

and Jones, 1988; Jones et al., 1992). Deposits are ponded into the central parts of the basin with thickness increasing from 30 to 100 cm (Fig. 2). No sand or mud breaks are found in this part of the Moroccan Turbidite System (Fig. 6A and B).

Total grain-size distributions for Bed 5 within each of the three basins show significant variation (Fig. 4). Across the Agadir Basin, deposits are bimodal with modes at *ca* 10 μm and 100 μm and a deficiency of silt-sized sediment between *ca* 30 to 40 μm . Across the Madeira Abyssal Plain, deposits are significantly finer-grained compared to the Agadir Basin, and have a unimodal grain-size distribution comprising high frequencies between *ca* 15 μm and 35 μm . Across the Seine Abyssal Plain, deposits have a broadly unimodal grain-size distribution that is negatively skewed to values of *ca* 20 μm , albeit with significant abundances of grain sizes with modes of *ca* 100 to 200 μm .

Bed 7

This large-volume turbidite (*ca* 120 km³) comprises relatively thin (*ca* 5 to 15 cm), fine-grained sands with modal grain-size values of between *ca* 65 μm and 100 μm , which extend across the Agadir Basin, Madeira Channel System and Madeira Abyssal Plain (Fig. 2) (Wynn et al., 2002; Frenz et al., 2008; Stevenson et al., 2012). Almost all sand deposits are normally-graded ripple cross-laminated with no grain-size breaks (Fig. 8A).

In contrast, *Type IV grain-size breaks* are common throughout Bed 7 (Fig. 8B). Within the Agadir Basin they occur between normally-graded, ripple cross-laminated sand with modal grain sizes of *ca* 63 to 80 μm , overlain by relatively thick (*ca* 25 to 60 cm), graded, ungraded and contorted muds with modal grain-size values between *ca* 10 and 20 μm . Within the south-west parts of the Agadir Basin contorted muds are the most common facies overlying *Type IV grain-size breaks* (Fig. 8B). Across the Madeira Abyssal Plain deposits are generally fine-grained (*ca* 63 to 80 μm) and thicken progressively into the central parts of the basin (Fig. 2). No grain-size breaks are observed in this part of the Moroccan Turbidite System.

Total grain-size distributions for Bed 7 within the Agadir and Madeira Abyssal Plain are similar (Fig. 4). Across the Madeira Abyssal Plain, deposits have a unimodal distribution of *ca* 10 μm . Across the Agadir Basin, deposits have a slightly bimodal distribution with modes of *ca* 6 μm and 20 μm . Overall, Bed 7 is the finest-grained turbidite examined in this study.

Bed 11

This relatively small-volume turbidite ($ca\ 15\ km^3$) proximally comprises a thick, structureless, parallel laminated, normally-graded clean sand deposit ($ca\ 80\ cm$ thick) within the north-east Agadir Basin (Frenz et al., 2008). The bed rapidly thins to the south-west progressing into deposits composed of thin ($ca\ 10\ cm$) clean sands, which ultimately pinch out leaving normally-graded silt and mud deposits across most of the basin. *Type III grain-size breaks* are frequent within the upper parts of sand deposits but restricted to proximal localities (Fig. 9A); they occur between parallel laminated sands with modal grain-size values between $ca\ 100\ \mu m$ and $150\ \mu m$, overlain by structureless finer sand with modal grain-size values of $ca\ 60\ \mu m$ (Fig. 10, Core CD166/51).

Type IV grain-size breaks occur almost throughout Bed 11, where there is a grain-size transition from sand into mud (Fig. 9B). The majority of *Type IV grain-size breaks* found within Bed 11 are overlain by ungraded, structureless turbidite mud $ca\ 10$ to $20\ cm$ thick. However, in some deposits graded or contorted muds can overlie the grain-size break (Fig. 10, Core D13073). Two deposits within the Seine Abyssal Plain have exceptionally thin sands (2 to $9\ cm$) that normally grade into silts and muds.

Total grain-size distributions for Bed 11 within the Agadir Basin and Seine Abyssal Plain are different (Fig. 4). Across the Agadir Basin, deposits show a bimodal distribution with modes of $ca\ 20\ \mu m$ and $200\ \mu m$, and a deficiency in grain-sizes between $ca\ 30$ to $40\ \mu m$. Across the Seine Abyssal Plain, deposits have a broadly unimodal grain-size distribution, which has high frequencies from $ca\ 10\ \mu m$ to $100\ \mu m$ and a modal peak at $ca\ 25\ \mu m$.

Bed 12

This large-volume bed ($>180\ km^3$) is one of the biggest turbidites emplaced across the Moroccan Turbidite System over the past $200\ ka$ (Wynn et al., 2002; Frenz et al., 2008). It comprises relatively tabular, 60 to $120\ cm$ thick, structureless, planar- and ripple cross-laminated sheet sands that extend across the Seine Abyssal Plain, Agadir Basin, across the Madeira Channel System, and into the Madeira Abyssal Plain (Fig. 2; Wynn et al., 2002; Frenz et al., 2008; Stevenson et al., 2012). *Type II grain-size breaks* are occasionally found close to the mouth of the Agadir Canyon (Fig. 11A) and occur between inversely graded sands with modal values of $ca\ 400\ \mu m$, overlain by ungraded finer sand with modal values of $ca\ 150\ \mu m$ (Fig. 12, Core CD166/51).

Type IV grain-size breaks are found throughout Bed 12 (Fig. 11B). Across the Agadir Basin *Type IV grain-size breaks* occur between sand (*ca* 70 μm) overlain by a relatively thin (*ca* 10 to 15 cm), ungraded structureless mud (*ca* 10 to 15 μm ; Fig. 12, Core CD166/24). Within the Seine Abyssal Plain, *Type IV grain-size breaks* are overlain by thicker muds with graded and contorted bases (Fig. 12, Core D13073). Deposits within the Madeira Abyssal Plain are normally-graded, very fine-grained sands, silts and muds (Fig. 12 Core D11813). Bed 12 develops from thin-bedded (5 to 10 cm) sands at the terminus of the Madeira Channel System in the north-east, to thick deposits (*ca* 200 to 500 cm) of ponded mud with silt-rich, normally-graded bases within the central parts of the basin (Fig. 2) (Jones et al., 1992; Rothwell et al., 1992; Weaver et al., 1992). Only four core sites, proximal to the mouth of the Madeira Channel System, record *Type IV grain-size breaks*, which are overlain by ungraded, graded or contorted mud (Fig. 11B).

Total grain-size distributions for Bed 12 within the Seine Abyssal Plain, Agadir Basin and Madeira Abyssal Plain are different (Fig. 4). Grain-size distributions within the Agadir Basin are bimodal with a weak mode of *ca* 10 μm and a strong mode of *ca* 90 μm , and a deficiency of grain sizes between *ca* 20 μm and 30 μm . Across the Seine Abyssal Plain, deposits have similar bimodal grain-size distributions with modes of *ca* 10 μm and 150 μm . Across the Madeira Abyssal Plain, deposits have a negatively skewed unimodal grain-size distribution with a mode of *ca* 10 μm but with relatively high frequencies of grain sizes from *ca* 6 to 40 μm .

DISCUSSION

In this section the different mechanisms by which grain-size breaks form are discussed and evaluated for the grain-size breaks observed in the Moroccan Turbidite System.

Bimodal grain-size distribution within flows

An idealised turbidite deposit comprises coarse sediment at the base that progressively fines upwards, i.e. from sand, to silt and then clay (e.g. Bouma, 1962). Flows that produce these beds must contain the full range of coarse to fine grain sizes. Flows with strongly bimodal grain-size distributions, in which the intermediate grain sizes are entirely absent (or in very low abundance), will produce deposits that have sharp vertical transitions in grain size, i.e. grain-size breaks (Fig. 13A) (Kuenen, 1953; Bouma, 1962; Kneller and

McCaffrey, 2003; Kane et al., 2007). Grain-size breaks produced in this manner would form across grain sizes that are absent (or in low abundance) within the flow.

Type I and II grain-size breaks are found in Beds 5 and 12 within the Agadir Basin (Figs 6A and 11A); they occur between coarse sand (*ca* 900 to 1000 μm) overlain by finer grained structureless sand (*ca* 100 to 200 μm). The total grain-size distributions for Beds 5 and 12 within the Agadir Basin show that both beds have smoothly increasing abundances of grain sizes from *ca* 1000 to 200 μm . Although coarse-grained material is in relatively low abundance compared to the total grain-size distribution, there is not a relative deficiency in grain sizes between *ca* 1000 μm and 200 μm (Fig 4). Therefore, grain-size breaks were not formed by a low abundance of grain sizes between *ca* 1000 μm and 200 μm within the parent flow. *Type IV grain-size breaks* are present in every bed, occurring between sand with modal values of *ca* 100 to 70 μm , overlain by mud with modal values of *ca* 10 to 20 μm . Beds 3, 7 and 11 have unimodal distributions that include significant abundances of grain sizes between *ca* 10 μm and 20 μm (Fig. 4). Beds 5 and 12 have bimodal distributions with deficiencies of grain sizes between *ca* 10 μm and 20 μm within the Agadir Basin. However, the grain sizes that are deficient within the Agadir Basin are found *ca* 1000 km down slope within the Madeira Abyssal Plain (Fig. 4). Therefore, *Type IV grain-size breaks* were not produced from grain sizes between 20 μm and 70 μm being in low abundance within the parent flows.

Flow reflection

Grain-size breaks can be caused by reflection of turbidity currents at basin margins or at other obstacles (Fig. 13B) (Pickering and Hiscott, 1985; Kneller et al., 1991; Kneller and McCaffrey, 1999). Laboratory experiments illustrate the dynamics of flow reflection with topography. In turn, studies have attempted to link these dynamics with certain turbidite facies. Weak reflections (less powerful than the primary flow) are propagated along density interfaces above the bed (Pantin and Leeder, 1987), which may produce ripples at high angles to the primary flow direction (Fig. 13B) (Kneller et al., 1991; Kneller et al., 1997; Kneller and McCaffrey, 1999). In contrast, strong reflections (more powerful than the primary flow) can undercut the primary flow and propagate along the bed, which may produce multiple fining upward sequences within a single bed separated by sharp grain-size breaks (Fig. 13B) (Kneller et al., 1991; Rothwell et al., 1992; Edwards et al., 1994; Haughton, 1994; Kneller and McCaffrey, 1999; Remacha et al., 2005). However, no such multiple fining upward sequences that are separated by grain-size breaks are observed in Beds 3, 5, 7, 11 and 12.

Therefore, it is unlikely that flow reflection generated grain-size breaks found across the Moroccan Turbidite System.

Flow separation due to topographic obstacles

Sinclair and Cowie (2003) proposed that grain-size breaks could form when a turbidity current encounters a topographic barrier that diverts only the lower part of the flow (Fig. 13C). The upper and finer-grained part of the flow thus follows a different path to the coarser-grained lower part of the flow. The Moroccan Turbidite System lacks suitable topographic barriers for this process to operate, with deposition occurring on low-gradient open slopes or basin plains. Hence, it is very unlikely that this mechanism formed the grain-size breaks in the Moroccan System turbidites.

Internal grain-size and concentration boundary within a flow

Gladstone and Sparks (2002) attributed grain-size breaks in turbidites to deposition from a flow comprising two distinct layers: a body and an overlying wake (Fig. 14A). In this model, both body and wake are relatively dilute and fully turbulent. These authors inferred that a sharp discontinuity in grain size occurred within the flow at the boundary between body and wake. The grain-size break within the deposit was attributed to an abrupt change from deposition by the body to deposition from the wake. There are two significant problems with this type of explanation for grain-size breaks.

First, unless the flow deposits very quickly or *en masse*, the vertical structure of the flow will not be preserved as the vertical structure of the deposit. A deposit that builds up incrementally will preserve the longitudinal (front to tail) structure of the flow (Kneller and Branney, 1995). Hence, this mechanism does not explain grain-size breaks that occur in association with incrementally aggraded facies. For example, parallel and/or ripple-cross laminated sands found within Beds 3, 5, 7, 11 and 12, were deposited incrementally (Best and Bridge, 1992; Kneller and Branney, 1995; Sumner et al., 2008; Baas et al., 2011). Hence, *Type II and III grain-size breaks* occurring within these facies are likely to be a product of abrupt lateral variations within a flow, rather than the vertical structure of the flow (Mutti et al., 2002; Kneller and McCaffrey, 2003).

Second, the Gladstone and Sparks (2002) hypothesis was based on the fact that a flow with relatively low sediment concentration may develop a sharp internal boundary on visual observations of saline density currents (Britter and Simpson, 1978; Hallworth et al., 1996).

Experimental analyses of dilute particle-laden density flows have not observed such sharp vertical boundaries in grain size and concentration (Kneller and Buckee, 2000; Felix, 2002; Kneller and McCaffrey, 2003; Choux et al., 2005; Felix et al., 2005; Manica, 2012). In these experiments turbulent mixing tends to produce gradational changes in grain size and concentration away from the bed. However, sharp vertical changes in grain size and sediment concentration have been observed in laboratory experiments involving relatively high sediment concentrations (Postma et al., 1988; Marr et al., 2001; Mohrig and Marr, 2003; Ilstad et al., 2004; Felix et al., 2005; Manica, 2012). In these experiments, a sharp density interface develops between an overlying dilute, finer grained turbulent suspension and a high-concentration basal flow in which turbulence is suppressed. High-concentration flows (including debris flows) can deposit *en masse* rather than incrementally (e.g. Manica, 2012). Thus, deposits that were produced by high-concentration parts of a flow could have grain-size breaks generated via sharp vertical concentration boundaries (Fig. 14A).

Type I grain-size breaks are found wherever poorly sorted, coarse sand-sized sediment is deposited (for example, Figs 7 and 12; Beds 5 and 12, respectively). Such coarse-grained sediment is likely to be transported within high-concentration traction carpets at the base of the flow, whereby particles are supported by inter-grain interactions rather than fluid turbulence (Hsu, 1959; Dzulynski and Sanders, 1962; Postma et al., 1988; Hiscott, 1994; Sohn, 1997; Vrolijk and Southard, 1997). The boundary between the basal layer, which can transport large grains, and the overriding flow, which cannot transport large grains, is sharp (Postma et al., 1988). Due to the high concentrations of sediment within the basal layer, deposition occurs rapidly. This preserves the vertical structure of the flow (at the base) and the sharp internal boundary between basal layer and overriding flow. *Type I grain-size breaks* probably are produced from such a sharp internal boundary; separating a very high-concentration basal layer and an overriding lower concentration suspension.

Mud-rich sands found overlying relatively clean sands within Bed 5 are interpreted to be linked-debrite deposits, produced from a high-concentration turbidity current. This turbidity current had a relatively high proportion of mud near to the bed, meaning that when it decelerated (with a concomitant reduction in shear stresses) cohesive bonds could be established and transformed parts of the turbidity current into a debris flow, which deposited *en masse* across the Agadir Basin (Talling et al., 2007c; Sumner et al., 2009; Wynn et al., 2010; Sumner et al., 2012; Talling et al., 2012a, b). *Type V grain-size breaks* occurring

between mud-rich structureless sand overlain by turbidite mud were most probably generated from a sharp concentration boundary within the parent flow; separating a cohesive debris flow and an overriding turbulent suspension. With time and distance from source, flow stratification will become stronger (Choux et al., 2005; Felix et al., 2005; Kane and Pontén, 2012) which is likely to produce sharper concentration profiles and make grain-size breaks more common. This explains why *Type V grain-size breaks* are rare in relatively proximal linked-debrite deposits yet exclusively overlie relatively distal linked-debrite deposits (Fig. 7B).

Fluctuations in flow capacity and competence

Kneller and McCaffrey (2003) attributed grain-size breaks to longitudinal velocity and concentration gradients within the parent flow (Fig. 14B). Proximally, a flow is likely to have strong variations in velocity, concentration and grain size along its length (disorganized). Theoretical analysis and experimental results show that capacity (the amount of particles that can be supported in a flow) increases with higher shear velocities and turbulence intensities, and within flows transporting finer grain sizes (Hiscott, 1994; Huppert et al., 1995; Orlin and Gulliver, 2003). Therefore, the flow will be unsteady as it passes over a fixed point, meaning that its capacity will temporally fluctuate relative to its sediment load. This effect can produce periods of deposition followed by periods of bypass and/or erosion of pre-existing deposits, at which point a grain-size break is produced (Kneller and McCaffrey, 2003). This mechanism is now discussed in terms of temporal and spatial changes in flow capacity.

Temporal changes in flow capacity and sediment load

Temporal changes in flow capacity require flows to be unsteady, either waxing or waning (Fig. 14B). Temporal changes in flow capacity will manifest themselves within incrementally aggraded deposits as inversely-graded sands for waxing flows and normally-graded sands for waning flows (Kneller and Branney, 1995). In addition, the proportion of fines within inversely-graded deposits, produced from waxing flows, should decrease upwards, reflecting decreasing rates of aggradation from the flow (Sylvester and Lowe, 2004; Kane et al., 2009). Theoretically, unsteadiness will decrease with distance from source because the flow organizes itself longitudinally, with faster moving parts of the flow (body) overtaking slower moving parts of the flow (head) (Walker, 1967; Kneller and McCaffrey, 2003). Hence, relatively distal turbidites generally have normally-graded vertical profiles,

whereas more proximal turbidites can show complex inverse to normal vertical grading profiles.

Within this study, *Type II grain-size breaks* occur between inversely-graded sands (with a contemporaneous decrease in silt content) overlain by finer sand, and are only found close to the mouth of the Agadir Canyon. Their association with inversely-graded sands indicates these grain-size breaks were most probably generated from waxing flows, which became sufficiently energetic to erode the pre-existing deposit (Talling et al., 2007a; Kane et al., 2009; Sumner et al., 2012), before recommencing deposition with a finer grain size.

The experiments of Sumner et al. (2008) have observed depositional hiatuses within flows temporally decelerated at a constant rate (waning). Initially, aggradation rates were relatively high with deposition of structureless and planar laminated sands; this was followed by a period of non-deposition and sometimes erosion/reworking of the pre-existing deposit. Deposition recommenced under much lower aggradation rates, forming a strongly graded deposit (Sumner et al., 2008). The change in aggradation rate across the hiatus may relate to the amount of hindered settling particles experience during deposition, or a change in settling regime from capacity to competence, i.e. the largest particle size that can be transported by the flow (Kneller and McCaffrey, 2003; Sumner et al., 2012; Talling et al., 2012a).

Type III grain-size breaks occur between parallel laminated sands overlain by better-sorted sands with strong normal grading (Fig. 10, Core CD166/51). Facies overlying and underlying *Type III grain-size breaks* in the Moroccan Turbidite System are similar to deposits formed before and after a depositional hiatus in the experiments of Sumner et al., (2008). Therefore, *Type III grain-size breaks* are interpreted here as a product of a flow switching between capacity to competence-induced deposition, which generates a depositional hiatus beneath a constantly waning flow (Fig. 14B).

Spatial changes in flow capacity and sediment load

Erosion, entrainment and deposition of sediment, entrainment of ambient fluid, and changes in slope will determine how a flow evolves (spatially), as it travels across the sea floor. Spatial changes in capacity and sediment load within the flow may generate grain-size breaks, even when the flow is temporally steady along its entire length (Kneller and McCaffrey, 2003; Eggenhuisen and McCaffrey, 2009). In this scenario, the front of the flow must be oversaturated with sediment and depositional, whilst the trailing body of the flow

must be undersaturated with sediment and bypassing. This longitudinal flow organisation is a continuous process because the head will always be subject to more entrainment of ambient fluid than the body (Kneller and Buckee, 2000, and references therein). However, the strongest variations in capacity between head and body are likely to occur close to source, before the flow has had time to equilibrate its velocity and sediment load (Kneller and Buckee, 2000; Kneller and McCaffrey, 2003; McCaffrey et al., 2003; Choux et al., 2005). Spatial changes in flow capacity and sediment load is a plausible mechanism by which grain-size breaks can form within an incrementally aggrading sand deposit. If coarse sand deposits found in Beds 5 and 12 were deposited incrementally, it is most likely that *Type I grain-size breaks* were produced via this mechanism.

Type IV grain-size breaks comprising clean sand overlain by a range of turbidite mud facies, occur throughout most of the Moroccan Turbidite System. Normal grading immediately underlying the grain-size breaks indicates that the parent flows were waning (Kneller and Branney, 1995). Potentially, these grain-size breaks were produced by spatial and/or temporal fluctuations in flow capacity as outlined above. However, the mechanism does not explain why *Type IV grain-size breaks* occur so consistently between fine sand with modal grain sizes of *ca* 70 to 100 μm , overlain by mud with modal grain sizes of *ca* 10 to 20 μm , irrespective of their proximity to source. Rather, it would be expected that higher flow velocities, proximal to source and on steeper areas of the sea floor, would produce *Type IV grain-size breaks* with a larger 'jump' in grain size; compared with slower moving parts of the flow, in more distal and/or flatter areas of the sea floor. Indeed, the opposite trend is found within Bed 12, where sharp *Type IV grain-size breaks* occur across flatter areas of the Agadir Basin, whilst normally-graded deposits occur across the steeper areas (Fig. 15). For these reasons both spatial and, temporal fluctuations in capacity could not generate the *Type IV grain-size breaks* observed in the Moroccan Turbidite System.

Development of fluid mud layers

This section first describes a conceptual model by which clay-rich suspensions develop cohesive fluid mud layers which, in turn, can produce *Type IV grain-size breaks* from a turbidity current. Second, the structure of clay-rich suspensions and the controls on their rheology are discussed, which are then related to vertical grading profiles within turbidite mud deposits. Finally, the depositional architecture of fluid muds and the distribution of *Type IV grain-size breaks* are discussed in relation to sea floor topography.

Towards the rear of a turbidity current, mud concentrations are relatively high and shear velocities at a minimum, allowing fine-grained silt and clay particles to settle out from suspension (Fig. 14C). Due to flocculation of clay particles, silt and clay may initially settle towards the bed at similar shear velocities (Whitehouse et al., 2000, and references therein). Continued settling of clay flocs from the overlying suspension increases the clay concentration near to the bed. This will initially hinder the settling of grains from above via a number of processes, including particle-induced return flow, particle-particle collision and interaction, increased viscosity, and reduced gravity (e.g. Winterwerp and van Kesteren, 2004). At sufficiently high concentrations ($> ca 10 \text{ g l}^{-1}$) the flocs suppress turbulence and the fluid achieves yield strength, similar to fluid muds observed in estuarine and coastal settings (McAnally et al., 2007a, b). The fluid mud layer hinders the settling of both clay flocs and non-cohesive silt grains, settling from the overlying suspension (Berlamont et al., 1993; Torfs et al., 1996; Cuthbertson et al., 2008; Dankers et al., 2008). The fluid mud layer is able to support grains that would otherwise settle out from a turbulent flow and bypasses these grains down slope (Fig. 14C). Ultimately, continued deceleration from the flow allows the fluid mud layer to deposit *en masse* via frictional freezing onto the bed, which produces deposits of ungraded, structureless turbidite mud (Piper, 1972, 1978; McCave and Jones, 1988; Jones et al., 1992; Sumner et al., 2009; Talling et al., 2012a).

Type IV grain-size breaks are interpreted to be generated by this process. In theory when a suspension containing a sufficient proportion of clay settles towards the bed, it will always produce a cohesive mud layer. This may explain the widespread occurrence of *Type IV grain-size breaks* across the Moroccan Turbidite System.

Competence of fluid mud layers

Fluid mud layers occur when mud concentrations exceed *ca 10 g/l* and interactions between cohesive particles lead to hindered settling. Fluid muds measured in shallow marine settings can exceed concentrations of *ca 4%* (*ca 100 g/l*) (Trowbridge and Kineke, 1994; Kineke and Sternberg, 1995; Wright et al., 2001; McAnally et al., 2007b) and can contain 20 to 60% of silt-sized particles, and occasionally support a few percent of fine sand (McAnally et al., 2007b). A fluid mud yield strength of *ca 0.2 to 0.02 Pa* would be sufficient to support non-cohesive quartz grains with diameters between $10 \mu\text{m}$ and $100 \mu\text{m}$ (Hampton, 1975; Amy et al., 2006). Mud suspensions achieve these yield strengths at volume concentrations of

ca 3 to 11%, which is largely dependent on the type of clay present in the suspension (Berlamont et al., 1993; Coussot and Piau, 1994; Coussot, 1995; McAnally et al., 2007b). Therefore, it is reasonable that a fluid mud layer could have sufficient yield strength to prevent deposition of the grain sizes (ca 10 μm to ca 100 μm) missing across *Type IV grain-size breaks*, and bypass them to distal parts of the Moroccan Turbidite System (for example, Fig. 4).

Vertical structure of cohesive mud flows and their deposits

Baas et al. (2009) constructed a phase diagram for turbulent, transitional and laminar clay-laden open channel flows; these experiments demonstrate that the vertical turbulence structure within the flow was determined by shear velocity and clay concentration (Fig. 16). Increasing the proportion of clay in a flow led to five different flow types: (i) turbulent flow, which is turbulent throughout its depth; (ii) turbulence-enhanced flow; (iii) lower transitional plug flow, comprising a lower turbulent region and a thinner overlying laminar plug; (iv) upper transitional plug flow, which has a thin turbulent underlayer overlain by a thicker laminar plug; and (v) quasi-laminar plug flow, comprising a laminar plug that moves on a thin shear layer (Baas et al., 2009). Further open channel experiments by Baas et al. (2011), using mixed cohesive (clay)/non-cohesive (sand and silt) sediment suspensions, showed that these flow types each produced distinct types of deposit (Fig. 16). ‘Turbulent Flow’ and ‘Turbulent Enhanced Transitional Flow’ regimes produced bipartite deposits, consisting of a sandy layer overlain by a silty layer. ‘Lower Transitional Plug Flow’ and ‘Upper Transitional Plug Flow’ regimes generated sandy deposits directly overlain by a fluid mud with enough yield strength to support silt grains. With increasing clay concentration the fluid mud layer became thicker with higher yield strengths; meaning that it could support larger and larger non-cohesive grains, which produced thicker ungraded mud caps with a coarser component of silt. Within the ‘Quasi-Laminar Plug Flow’ regime the fluid mud layer achieved sufficient yield strength to partially support fine sand, and then with increasing concentrations fully support all sandy grain sizes in the suspension. This resulted in deposits of ungraded mud; initially with the coarsest sand grains settled towards the bottom, then progressing to an ungraded mud with all available grain-sizes scattered throughout (Baas et al., 2011). Similar transitional flow behaviour was observed by Manica (2012) who used a lock-exchange methodology to model small-scale gravity currents carrying a range of cohesive/non-cohesive sediment mixtures. With increasing proportions of clay the flows progressed from inertia-

dominated (turbulent) to viscous-dominated flows, and ultimately became quasi-laminar plug flows (Baas et al., 2009) with sufficient yield strength to support all available grain sizes (Manica, 2012).

Because similar behaviour is observed in both clay-rich open channel flows and scaled clay-rich gravity currents, the present authors consider the experiments of Baas et al. (2009; 2011) to be representative of conditions experienced by particles within a decelerating clay-rich suspension toward the rear of a turbidity current: increasing clay content and decreasing shear stresses near to the bed.

The five flow types of Baas et al. (2009) and their associated deposits (Baas et al., 2011) are used to interpret the range of vertical grading profiles found within turbidite muds across the Moroccan Turbidite System (Fig. 16). Turbulent and turbulence-enhanced flows will produce deposits that are graded, potentially with sedimentary structures throughout. Lower and upper transitional plug flows will progressively hinder the settling of non-cohesive grains, producing deposits that have graded silty bases overlain by ungraded mud. With increasing clay concentration the graded bases become thinner and the overlying mud cap thicker. Low yield strength quasi-laminar plug flows will produce deposits of ungraded mud with possible pseudonodules of silt/very fine sand sorted towards the base. High yield strength quasi-laminar plug flows will produce deposits of ungraded mud with possible pseudonodules of silt/fine sand scattered throughout. The interpretation herein of mud cap facies and grading patterns has similarities with recent work that has related the vertical structure of flows, transitional between non-cohesive and cohesive rheologies, to the vertical structure of linked debrite-turbidite deposits or hybrid beds (Sumner et al., 2009; Baas et al., 2011; Kane and Pontén, 2012)

Spatial variability in fluid mud

Once a fluid mud layer has formed, toward the rear of a turbidity current, the balance of cohesive and turbulent forces within the flow is likely to be affected by changes in sea floor gradient. Increases in slope will increase flow velocity and near bed shear stresses, which will promote a more turbulent flow type. Decreases in slope will have the opposite effect, promoting a more cohesive (viscous-dominated) flow type.

An association between slope and *Type IV grain-size breaks* is found in the deposits of Bed 12 along the axis of the Agadir Basin (Fig. 15). Initially, *Type IV grain-size breaks*

overlain by ungraded structureless mud are found across the relatively flat north-east parts of the Agadir Basin. Progressing south-west along the axis of the basin (i.e. distally) there is an increase in slope from *ca* 0.01° to 0.03°. Although subtle, the relative change in slope is significant (more than double). Here, a core site shows Bed 12 to have a deposit that is normally-graded between sand and mud. Continuing south-west, the slope decreases to *ca* 0.016°, where *Type IV grain-size breaks* are found overlain by turbidite mud with normally-graded and contorted bases. This down flow pattern of *Type IV grain-size breaks* is interpreted to be the product of cohesive fluid mud hindering the settling of non-cohesive grains and bypassing them down slope. As the fluid mud accelerated over the increased slope it transformed into a turbulent flow that could not support the non-cohesive grains within it, enabling them to deposit onto the bed. As the fluid mud travelled further down slope onto flatter sea floor, a cohesive plug flow could re-establish, which hindered the settling of non-cohesive grains.

Models for the generation of grain-size breaks

The flow processes that can form grain-size breaks are spatially and temporally variable. Here a spatial and temporal framework is presented describing the generation of grain-size breaks (*Types I to IV*) within an idealized bed (Fig. 17A). The flow processes responsible for generating each type of grain-size break are illustrated in Figure 17B. For reference, different points along the flow pathway are labelled '1' to '5' whilst the time taken for the flow to pass over a fixed point is labelled 'a' to 'f' (see Fig. 17A and B). To complement Fig. 17A and B, Fig. 18 shows how the grain-size breaks are distributed within a simple bed.

Type I grain-size breaks are produced first from rapid deposition of high-concentration basal layers (Fig. 17A and B; 1a and 2a) (Postma et al., 1988; Vrolijk and Southard, 1997). This type of grain-size break is restricted to relatively proximal localities (Fig. 18). Next *Type II grain-size breaks* are produced whilst the flow is waxing/waning and its capacity is fluctuating compared to its sediment load (Fig. 17A and 17B; 1c). These types of grain-size break are absent distally as the flow organizes itself with distance from source (Figs 17B and 18). Next, *Type III grain-size breaks* are generated as the flow decelerates and switches from capacity-induced to competence-induced deposition. Such grain-size breaks are likely to be restricted to relatively proximal locations (Fig. 18). *Type IV grain-size breaks* are produced by fluid mud bypassing grains down slope (Fig. 17A and B; 1e, 3d, 4c). This

type of grain-size break occurs almost everywhere representing widespread generation of late-stage fluid mud layers. Notable exceptions are in very distal localities, at the limit of sandy deposition, and in topographic low points (proximal or distal) where mud has ponded (Fig. 18).

Type V grain-size breaks are produced via *en masse* deposition from a cohesive flow (Fig. 17C). This type of grain-size break is most frequent in distal localities because vertical stratification within the flow increases away from source, which generates a sharper internal concentration profile within the flow (Figs 17C and 18) (Choux et al., 2005; Felix et al., 2005; Kane and Pontén, 2012). However, with increasing yield strength a cohesive flow is likely to develop stronger (and sharper) internal concentration boundaries (Marr et al., 2001; Mohrig and Marr, 2003; Ilstad et al., 2004). Therefore, *Type V grain-size breaks* are likely to be more frequent and occur more proximally within higher yield strength flows.

Grain-size breaks in other turbidite sequences

Modern turbidite systems

Lebreiro et al. (1997) provide a detailed analysis of grain-size trends within Quaternary turbidites in the Horseshoe Abyssal Plain offshore from the Iberian Margin. Grain-size breaks between fine sand and mud are found throughout the basin (Lebreiro et al., 1997). However, the magnitude of the grain-size breaks (10 to 30 μm) is somewhat less than that seen in *Type IV grain-size breaks* within the Moroccan Turbidite System (10 to 100 μm). This is probably due to a lack of coarse-grained sediment within Horseshoe Abyssal Plain turbidites, which are composed primarily of silt and mud (Lebreiro et al., 1997).

Migeon et al. (2001) identified two types of grain-size break in recent turbidites on the southern levée of the Var Fan in the Mediterranean Sea. The first type of grain-size break occurred between normally-graded ripple cross-laminated sand, overlain by ungraded structureless turbidite mud (facies I and II of Migeon et al, 2001). The change in modal grain size across these grain-size breaks is *ca* 10 to 100 μm ; similar to *Type IV grain-size breaks* found across the Moroccan Turbidite System. Migeon et al., (2001) interpret this type of grain-size break as localized flow acceleration over the crest of sediment waves. However, similar (Type IV) grain-size breaks found in the Moroccan Turbidite System occur within relatively flat basin-plain settings that do not have sediment wave fields. Therefore, the

present authors propose grain-size breaks between clean sand and ungraded turbidite mud within the Var Fan could be a product of fluid mud bypassing sediment down slope, as interpreted for the Moroccan Turbidite System. The second type of grain-size break recognized by Migeon et al., (2001) occurred between mud-rich sand with mud clasts, overlain by ungraded structureless turbidite mud (facies IV). These are similar to *Type V grain-size breaks* found in the Moroccan Turbidite System, occurring between mud-rich sand overlain by ungraded turbidite mud. The present authors concur with Migeon et al., (2001) that this type of grain-size break is generated by a strong vertical concentration profile within a cohesive flow, which deposits *en masse* (i.e. a debris flow).

Ancient turbidite systems

Kane et al. (2009) examined internal erosion surfaces within turbidites of the Pendle Grit Formation, Northern England. These authors reported inversely-graded turbidites with contemporaneous decreasing clay content to have internal erosion surfaces, which resulted in a sharp grain-size break typically overlain by coarser sand. In the Moroccan Turbidite System, *Type II grain-size breaks* have a similar vertical grain-size profile, albeit that *Type II grain-size breaks* are overlain by finer grained sand. The present authors concur with Kane et al. (2009) that this type of grain-size break is the result of flow unsteadiness (waxing/waning) generating periods of deposition and erosion/bypass over time.

Eggenhuisen et al. (2011) examined turbidite beds of the Oligocene Macigno Formation, north-west Italy. These authors documented grain-size breaks occurring between structureless and parallel laminated sand, overlain by finer-grained ripple cross-laminated or contorted sand, similar to *Type III grain-size breaks* found within the Moroccan Turbidite System. In addition, the graphic logs presented in the Eggenhuisen et al. (2011) study show grain-size breaks occurring between sand and mud in almost every bed, analogous to *Type IV and V grain-size breaks* found in the Moroccan Turbidite System.

Individual basin-plain turbidites have been correlated within the Marnoso Arenacea Formation, Northern Apennines, Italy (Amy et al., 2005; Amy and Talling, 2006; Talling et al., 2007a, b; Sumner et al., 2012; Talling et al., 2012). Their facies and grain-size distributions have been mapped in both across flow and down flow directions. A range of different grain-size breaks have been reported from these beds: (i) grain-size breaks between sand overlain by finer-grained ripple cross-laminated sand, restricted to proximal localities;

(ii) grain-size breaks between sand and mud, which occur almost everywhere; and (iii) grain-size breaks between mud-rich structureless sand overlain by mud, which only occur in distal localities (Gladstone and Sparks, 2002; Amy and Talling, 2006; Talling et al., 2007a, b; Sumner et al., 2012). These grain-size breaks have similar facies associations and spatial distributions to the *Type III, IV and V grain-size breaks* found in the Moroccan Turbidite System, respectively. Indeed, correlation of individual beds demonstrates that missing grain sizes were bypassed and deposited down slope (Sumner et al., 2012), analogous to observations made for beds in the Moroccan Turbidite System (Fig. 4). Lateral correlation of turbidites in the Eocene Hecho Group, Spanish Pyrenees, reveals a similar phenomenon with *Type IV grain-size breaks*, where missing grain sizes have been bypassed and deposited down slope (Remacha et al., 2005).

The systems outlined above are by no means exceptional. Grain-size breaks, similar to *Types I, II, III, IV and V* found in the Moroccan Turbidite System, have been reported in a variety of turbidite systems from around the world (see examples in Kuenen, 1953; Ksiazkiewicz, 1954; Bouma, 1962; Walker, 1967; Mutti, 1992; Sylvester and Lowe, 2004). In particular, *Type IV grain-size breaks*, between sand overlain by mud, appear almost everywhere, as a dominant feature in: levée deposits within the Upper Cretaceous Rosario Formation, Baja California, Mexico (Kane et al., 2007); unconfined turbidites within the Aberystwyth Grit Formation and Windermere Super Group, UK (Walker, 1967; Gladstone and Sparks, 2002 and references therein); and foreland basin turbidites within the Eocene–Oligocene Tavezyannaz Sandstone, south-east France (Sinclair and Cowie, 2003).

Conclusions

This study examines in detail the vertical and spatial distribution of grain-size breaks within five turbidites found across the Moroccan Turbidite System. Five types of grain-size break were found: *Type I* – occurred in proximal areas between coarse sand and finer grained structureless sand; *Type II* – occurred in proximal areas between inversely-graded sand overlain by finer-grained sand; *Type III* – occurred in proximal areas between sand overlain by ripple cross-laminated finer sand; *Type IV* – occurred system-wide between clean sand and mud; and *Type V* – occurred only in relatively distal areas between mud-rich (debrite) sand and mud.

Type I grain-size breaks are interpreted as a product of a sharp internal boundary between a hyper-concentrated basal layer (that is able to transport coarse sand) and a lower concentration overriding suspension (that is not able to transport coarse sand). *Types II and III* are interpreted as a product of spatial and temporal fluctuations in flow capacity, and/or flows switching from capacity-induced to competence-induced deposition. Indeed, the absence of these types of grain-size break distally supports the notion that flows organize themselves longitudinally with distance from source. *Type IV grain-size breaks* are interpreted to be the product of late-stage development of fluid mud, which hinders the settling of non-cohesive grains and bypasses them down slope. Grain-size analysis of the individual beds proximally (50 km) and distally (>1500 km) demonstrates that the missing grain sizes are found down slope, situated within thick ponded mud caps. Finally, *Type V grain-size breaks* are interpreted to be a product of a sharp vertical concentration boundary within the parent flow. *Type V grain-size breaks* are only found in distal linked-debrite deposits, whereas proximal linked-debrite deposits are normally-graded.

It is important to understand that late-stage settling of fines toward the rear of a decelerating turbidity current should always result in the generation a cohesive fluid mud layer near to the bed, unless there is insufficient clay to generate a cohesive fluid. Therefore, *Type IV grain-size breaks* should form a typical component of turbidite deposits, rather than occurring as an exception. A number of existing studies support this notion, suggesting that most turbidites have *Type IV grain-size breaks*.

ACKNOWLEDGEMENTS

We gratefully acknowledge the thorough and constructive reviews of Ian Kane, Peter Haughton, Rafael Manica and Associate Editor Jaco Baas, which have helped to improve the manuscript considerably. We gratefully acknowledge the MATLAB[®] programming support of Hector Marin-Moreno to present the grain-size distribution data as contour plots. The UK-TAPS Agadir Project was carried out with financial support from NERC and a hydrocarbon industry consortium comprising BHP Billiton, ConocoPhillips, ExxonMobil, Norsk Hydro and Shell. We are very grateful to all technical and scientific staff involved in the various cruises that collected data for this study, in particular those involved in Cruises CD166 and JC27.

REFERENCES

- Amy, L.A. and Talling, P.J.** (2006) Anatomy of turbidites and linked debrites based on long distance (120 x 30 km) bed correlation, Marnoso Arenacea Formation, Northern Apennines, Italy. *Sedimentology*, **53**, 161-212.161-212
- Amy, L. A., Talling, P. J., Peakall, J., Wynn, R. B. and Arzola Thynne, R. G.** (2005) Bed geometry used to test recognition criteria of turbidites and (sandy) debrites. *Sedimentary Geology*, **79**, 163-174.
- Amy, L.A., Talling, P.J., Edmonds, V.O., Sumner, E.J. and Lesueur, A.** (2006) An experimental investigation of sand-mud suspension settling behaviour: implications for bimodal mud contents of submarine flow deposits. *Sedimentology*, **53**, 1411-1434.1411-1434
- Baas, J.H., Best, J.L. and Peakall, J.** (2011) Depositional processes, bedform development and hybrid bed formation in rapidly decelerated cohesive (mud-sand) sediment flows. *Sedimentology*, **58**, 1953-1987.1953-1987
- Baas, J.H., Best, J.L., Peakall, J. and Wang, M.** (2009) A phase diagram for turbulent, transitional, and laminar clay suspension flows. *Journal of Sedimentary Research*, **79**, 162-183.162-183
- Berlamont, J., Ockenden, M., Toorman, E. and Winterwerp, J.** (1993) The characterization of cohesive sediment properties. *Coastal Engineering*, **21**, 105-128.105-128
- Best, J. and Bridge, J.** (1992) The morphology and dynamics of low amplitude bedwaves upon upper stage plane beds and the preservation of planar laminae. *Sedimentology*, **39**, 737-752.737-752
- Birkenmajer, K.** (1958) Oriented flowage casts and marks in the Carpathian Flysch and their relation to flute and groove casts. *Acta Geologica Polonica*, **8**, 117-148.117-148
- Bouma, A.H.** (1962) Sedimentology of some Flysch Deposits: A Graphic Approach to Facies Interpretation. *Elsevier*

Britter, R.E. and Simpson, J.E. (1978) Experiments on dynamics of a gravity current head. *Journal of Fluid Mechanics*, **88**, 223-233.

Brown, R.J. and Branney, M. (2004) Bypassing and diachronous deposition from density currents: Evidence from a giant regressive bed form in the Poris ignimbrite, Tenerife, Canary Islands. *Geology*, **32**, 445-448.

Choux, C.M.A., Baas, J.H., McCaffrey, W.D. and Haughton, P.D.W. (2005) Comparison of spatio-temporal evolution of experimental particulate gravity flows at two different initial concentrations, based on velocity, grain size and density data. *Sedimentary Geology*, **179**, 49-69.

Coussot, P. (1995) Structural similarity and transition from Newtonian to Non-Newtonian behavior for clay-water suspensions. *Physical Review Letters*, **74**, 3971-3974.

Coussot, P. and Piau, J.M. (1994) On the behavior of fine mud suspensions. *Rheologica Acta*, **33**, 175-184.

Cuthbertson, A., Dong, P., King, S. and Davies, P. (2008) Hindered settling velocity of cohesive/non-cohesive sediment mixtures. *Coastal Engineering*, **55**, 1197-1208.

Dankers, P.J., Sills, G.C. and Winterwerp, J.C. (2008) On the hindered settling of highly concentrated mud-sand mixtures. *Sediment and Ecohydraulics - INTERCOH*, **9**, 255-274.

Davies, T.L., VanNiel, B., Kidd, R.B. and Weaver, P.P.E. (1997) High-resolution stratigraphy and turbidite processes in the Seine Abyssal Plain, northwest Africa. *Geological Marine Letters*, **17**, 147-153.

de Lange, G.J., Jarvis, I. and Kuijpers, A. (1987) Geochemical characteristics and provenance of late Quaternary sediments from the Madeira Abyssal Plain, N. Atlantic. In: *Weaver, P.P.E., Thomson, J. (Eds.), Geology and Geochemistry of Abyssal Plains. Geol. Soc. Spec. Publ.*, **31**, 147-165.

Dzulynski, S. and Sanders, J.E. (1962) Current marks on firm mud bottoms. *Connecticut Academy of Science Transactions*, 42, 57-96.57-96

Edmonds, M. and Herd, R.A. (2005) Inland-directed base surge generated by the explosive interaction of pyroclastic flows and seawater at Soufriere Hills volcano, Montserrat. *Geology*, 33, 245-248.245-248

Edmonds, M., Herd, R.A. and Strutt, M.H. (2006) Tephra deposits associated with a large lava dome collapse, Soufriere Hills Volcano, Montserrat, 12-15 July 2003. *Journal of Volcanology and Geothermal Research*, 153, 313-330.313-330

Edwards, D.A., Leeder, M.R., Best, J.L. and Pantin, H.M. (1994) On experimental reflected density currents and the interpretation of certain turbidites. *Sedimentology*, 41, 437-461.437-461

Eggenhuisen, J.T., McCaffrey, W.D., Haughton, P.D.W. and Butler, R.W.H. (2011) Shallow erosion beneath turbidity currents and its impact on the architectural development of turbidite sheet systems. *Sedimentology*, 58, 936-959.936-959

Felix, M. (2002) Flow structure of turbidity currents. *Sedimentology*, 49, 397-419.397-419

Felix, M., Sturton, S. and Peakall, J. (2005) Combined measurements of velocity and concentration in experimental turbidity currents. *Sedimentary Geology*, 179, 31-47.31-47

Frenz, M., Wynn, R.B., Georgiopoulou, A., Bender, V.B., Hough, G., Masson, D.G., Talling, P.J. and Cronin, B.T. (2008) Provenance and pathways of late Quaternary turbidites in the deep-water Agadir Basin, northwest African margin. *International Journal of Earth Sciences*, 98, 721-733.721-733

Gladstone, C. and Sparks, R.S.J. (2002) The significance of grain size breaks in turbidites and pyroclastic density current deposits. *Journal of Sedimentary Research*, 72, 182-191.182-191

Hallworth, M.A., Huppert, H.E., Phillips, J.C. and Sparks, R.S.J. (1996) Entrainment into two-dimensional and axisymmetric turbulent gravity currents. *Journal of Fluid Mechanics*, **308**, 289-311.289-311

Hampton, M.A. (1975) Competence of fine-grained debris flows. *Journal of Sedimentary Petrology*, **45**, 834-844.834-844

Haughton, P.D.W. (1994) Deposits of deflected and ponded turbidity currents, Sorbas Basin, Southeast Spain. *Journal of Sedimentary Research Section A-Sedimentary Petrology and Processes*, **64**, 233-246.233-246

Haughton, P.D.W., Barker, S.P. and McCaffrey, W.D. (2003) 'Linked' debrites in sand-rich turbidite systems - origin and significance. *Sedimentology*, **50**, 459-482.459-482

Hiscott, R.N. (1994) Loss of capacity, not competence, as the fundamental process governing deposition from turbidity currents. *Journal of Sedimentary Research Section A-Sedimentary Petrology and Processes*, **64**, 209-214.209-214

Hiscott, R.N. (1994) Traction-carpet stratification in turbidites - Fact or Fiction? *Journal of Sedimentary Research Section A-Sedimentary Petrology and Processes*, **64**, 204-208.204-208

Hsu, J.K. (1959) Flute and groove-casts in the Prealpine Flysch, Switzerland. *American Journal of Science*, **257**, 529-536.529-536

Hunt, J.E., Wynn, R.B., Masson, D.G., Talling, P.J. and Teagle, D.A.H. (2011) Sedimentological and geochemical evidence for multistage failure of volcanic island landslides: A case study from Icod landslide on north Tenerife, Canary Islands. *Geochemistry Geophysics Geosystems*, **12**, 1-36.1-36

Huppert, H.E., Turner, J.S. and Hallworth, M.A. (1995) Sedimentation and entrainment in dense layers of suspended particles stirred by an oscillating grid. *Journal of Fluid Mechanics*, **289**, 263-293.263-293

Ilstad, T., Elverhoi, A., Issler, D. and Marr, J.G. (2004) Subaqueous debris flow behaviour and its dependence on the sand/clay ratio: a laboratory study using particle tracking. *Marine Geology*, **213**, 415-438.415-438

Jones, K.P.N., McCave, I.N. and Weaver, P.P.E. (1992) Textural and dispersal patterns of thick mud turbidites from the Madeira Abyssal Plain. *Marine Geology*, **107**, 149-173.149-173

Kane, I.A. and Hodgson, D.M. (2011) Sedimentological criteria to differentiate submarine channel levee subenvironments: Exhumed examples from the Rosario Fm. (Upper Cretaceous) of Baja California, Mexico, and the Fort Brown Fm. (Permian), Karoo Basin, S. Africa. *Marine and Petroleum Geology*, **28**, 807-823.807-823

Kane, I.A., McCaffrey, W.D. and Martinsen, O.J. (2009) Allogenic vs. Autogenic controls on megaflute formation. *Journal of Sedimentary Research*, **79**, 643-651.643-651

Kane, I.A., Kneller, B.C., Dykstra, M., Kassem, A. and McCaffrey, W.D. (2007) Anatomy of a submarine channel-levee: An example from Upper Cretaceous slope sediments, Rosario Formation, Baja California, Mexico. *Marine and Petroleum Geology*, **24**, 540-563.540-563

Kineke, G.C. and Sternberg, R.W. (1995) Distribution of fluid muds on the Amazon-Shelf. *Marine Geology*, **125**, 193-233.193-233

Kneller, B. and Buckee, C. (2000) The structure and fluid mechanics of turbidity currents: a review of some recent studies and their geological implications. *Sedimentology*, **47**, 62-94.62-94

Kneller, B., Edwards, D., McCaffrey, W. and Moore, R. (1991) Oblique reflection of turbidity currents. *Geology*, **19**, 250-252.250-252

Kneller, B.C., Bennett, S.J. and McCaffrey, W.D. (1997) Velocity and turbulence structure of density currents and internal solitary waves: potential sediment transport and the formation of wave ripples in deep water. *Sedimentary Geology*, **112**, 235-250.235-250

Kneller, B.C. and Branney, M.J. (1995) Sustained high-density turbidity currents and the deposition of thick massive sands. *Sedimentology*, **42**, 607-616.607-616

Kneller, B.C. and McCaffrey, W.D. (1999) Depositional effects of flow non-uniformity and stratification within turbidity currents approaching a bounding slope: deflection, reflection and facies variation. *Journal of Sedimentary Research*, **69**, 980-991.980-991

Kneller, B.C. and McCaffrey, W.D. (2003) The interpretation of vertical sequences in turbidite beds: The influence of longitudinal flow structure. *Journal of Sedimentary Research*, **73**, 706-713.706-713

Ksiazkiewicz, M. (1954) Graded and laminated bedded in the Carpathian Flysch. *Annales Societatis Geologorum Poloniae*, **22**, 399–449.399–449

Kuenen, P.H. (1953) Significant features of graded bedding. *AAPG Bulletin*, **37**, 1044-1066.1044-1066

Lebreiro, S.M., McCave, I.N. and Weaver, P.P.E. (1997) Late Quaternary turbidite emplacement on the Horseshoe abyssal plain (Iberian margin). *Journal of Sedimentary Research*, **67**, 856-870.856-870

Lowe, D.R. (1982) Sediment gravity flows .2. Depositional models with special reference to the deposits of high-density turbidity currents. *Journal of Sedimentary Petrology*, **52**, 279-298.279-298

Manica, R. (2012) Sediment gravity flows: Study based on experimental simulations. *Hydrodynamics - Natural Water Bodies, Prof. Harry Schulz (Ed.)*

Marr, J.G., Harff, P.A., Shanmugam, G. and Parker, G. (2001) Experiments on subaqueous sandy gravity flows: The role of clay and water content in flow dynamics and depositional structures. *Geological Society of America Bulletin*, **113**, 1377-1386.1377-1386

Masson, D.G. (1994) Late Quaternary turbidity current pathways to the Madeira Abyssal Plain and some constraints on turbidity current mechanisms. *Basin Research*, **6**, 17-33.17-33

McAnally, W.H., Friedrichs, C., Hamilton, D., Hayter, E., Shrestha, P., Rodriguez, H., Sheremet, A., Teeter, A. and Flu, A.T.C.M. (2007a) Management of fluid mud in estuaries, bays, and lakes. I: Present state of understanding on character and behavior. *Journal of Hydraulic Engineering-Asce*, **133**, 9-22.9-22

McAnally, W.H., Teeter, A., Schoellhamer, D., Friedrichs, C., Hamilton, D., Hayter, E., Shrestha, P., Rodriguez, H., Sheremet, A., Kirby, R. and Fl, A.T.C.M. (2007b) Management of fluid mud in estuaries, bays, and lakes. II: Measurement, modeling, and management. *Journal of Hydraulic Engineering-Asce*, **133**, 23-38.23-38

McCaffrey, W.D., Choux, C.M., Baas, J.H. and Haughton, P.D.W. (2003) Spatio-temporal evolution of velocity structure, concentration and grainsize stratification within experimental particulate gravity currents. *Marine and Petroleum Geology*, **20**, 851-860.851-860

McCave, I.N. and Jones, K.P.N. (1988) Deposition of ungraded muds from high-density non-turbulent turbidity currents. *Nature*, **333**, 250-252.250-252

McMaster, R.L. and Lachance, T.P. (1969) Northwestern African Continental Shelf Sediments. *Marine Geology*, **7**, 57-67.57-67

Migeon, S., Savoye, B., Zanella, E., Mulder, T., Faugeres, J.C. and Weber, O. (2001) Detailed seismic-reflection and sedimentary study of turbidite sediment waves on the Var Sedimentary Ridge (SE France): significance for sediment transport and deposition and for the mechanisms of sediment-wave construction. *Marine and Petroleum Geology*, **18**, 179-208.179-208

Mohrig, D. and Marr, J.G. (2003) Constraining the efficiency of turbidity current generation from submarine debris flows and slides using laboratory experiments. *Marine and Petroleum Geology*, **20**, 883-899.883-899

Mutti, E., Lucchi, F. and Roveri, M. (2002) Revisiting turbidites of the Marnoso Arenacea Formation and their Basin-Margin equivalents: Problems with classic models. *Excursion Guidebook, 64th EAGE Conferene and Exhibition*, 52.52

Orlins, J.J. and Gulliver, J.S. (2003) Turbulence quantification and sediment resuspension in an oscillating grid chamber. *Experiments in Fluids*, **34**, 662-677.662-677

Pantin, H.M. and Leeder, M.R. (1987) Reverse flow in turbidity currents - The role of internal solitons. *Sedimentology*, **34**, 1143-1155.1143-1155

Pearce, T.J. and Jarvis, I. (1992) Composition and provenance of turbidite sands - Late Quaternary, Madeira Abyssal Plain. *Marine Geology*, **109**, 21-51.21-51

Pearce, T.J. and Jarvis, I. (1995) High-resolution chemostratigraphy of Quaternary distal turbidites: a case study of new methods for the analysis and correlation of barre sequences. *In: Dunay, R.E., Hailwood, E.A. (Eds.), Non-Biostratigraphical Methods of Dating and Correlation. Geol. Soc. Spec. Publ.* , **89**, 107-143.107-143

Pickering, K.T. and Hiscott, R.N. (1985) Contained (reflected) turbidity currents from the Middle Ordovician Cloridorme Formation, Quebec, Canada - An alternative to the antidune hypothesis. *Sedimentology*, **32**, 373-394.373-394

Piper, D.J.W. (1972) Turbidite origin of some laminated mudstones. *Geological Magazine*, **109**, 115-&.115-&

Piper, D.J.W. (1978) Turbidite muds and silts on deepsea fans and abyssal plains. *In (eds. Stanley, D. J. and Kelling, G.) Sedimentation in submarine canyons, fans and trenches, Dowden, Hutchinsion and Ross*, 163-176.163-176

Postma, G., Nemeč, W. and Kleinspehn, K.L. (1988) Large floating clasts in turbidites: a mechanism for their emplacement. *Sedimentary Geology*, **58**, 47-61.47-61

Remacha, E., Fernandez, L.P. and Maestro, E. (2005) The transition between sheet-like lobe and basin-plain turbidites in the Hecho basin (South-Central Pyrenees, Spain). *Journal of Sedimentary Research*, **75**, 798-819.798-819

Rothwell, R.G., Pearce, T.J. and Weaver, P.P.E. (1992) Late Quaternary Evolution of the Madeira Abyssal Plain, Canary Basin, NE Atlantic. *Basin Research*, **4**, 103-131.103-131

Sinclair, H.D. and Cowie, P.A. (2003) Basin-floor topography and the scaling of turbidites. *Journal of Geology*, **111**, 277-299.277-299

Sohn, Y.K. (1997) On traction-carpet sedimentation. *Journal of Sedimentary Research*, **67**, 502-509.502-509

Stanley, D. (1982) Welded slump-graded sand couplets: evidence for slide generated turbidity currents. *Geo-Marine Letters*, **2**, 149-155.149-155

Stevenson, C.J., Talling, P.J., Wynn, R.B., Masson, D.G., Hunt, J.E., Frenz, M., Akhmetzhanov, A. and Cronin, B.T. (2012) The flows that left no trace: very large-volume turbidity currents that bypassed sediment through submarine channels without eroding the seafloor. *Marine and Petroleum Geology*, In Press.In Press

Stow, D.A. and Shamugam, G. (1980) Sequence of structures in fine-grained turbidites: Comparison of recent deep-sea and ancient flysch sediments. *Sedimentary Geology*, **25**, 23-42.23-42

Stow, D.A.V. and Bowen, A.J. (1978) Origin of lamination in deep-sea, fine-grained sediments. *Nature*, **274**, 324-328.324-328

Stow, D.A.V. and Piper, D.J.W. (1984) Deep-water fine-grained sediments: facies models. In: *Stow, D. A. V. and Piper, D. J. W. (eds), Fine-grained sediments: Deep-water processes and facies. The Geological Society*, 611-646.611-646

Sumner, E.J., Amy, L.A. and Talling, P.J. (2008) Deposit structure and processes of sand deposition from decelerating sediment suspensions. *Journal of Sedimentary Research*, **78**, 529-547.529-547

Sumner, E.J., Talling, P.J. and Amy, L.A. (2009) The deposits of flows transitional between turbidity currents and debris flow. *Geology*, **37**, 991-994.

Sumner, E.J., Talling, P.J., Amy, L.A., Wynn, R.B., Stevenson, C.J. and Frenz, M. (2012) Facies architecture of individual basin-plain turbidites: Comparison with existing models and implications for flow processes. *Sedimentology*, **59**, 1850-1887.

Sylvester, Z. and Lowe, D.R. (2004) Textural trends in turbidites and slurry beds from the Oligocene flysch of the East Carpathians, Romania. *Sedimentology*, **51**, 945-972.945-972

Talling, P.J., Amy, L.A., Wynn, R.B., Peakall, J. and Robinson, M. (2004) Beds comprising debrite sandwiched within co-genetic turbidite: origin and widespread occurrence in distal depositional environments. *Sedimentology*, **51**, 163-194.163-194

Talling, P.J., Amy, L.A. and Wynn, R.B. (2007a) New insight into the evolution of large-volume turbidity currents: comparison of turbidite shape and previous modelling results. *Sedimentology*, **54**, 737-769.737-769

Talling, P.J., Amy, L.A., Wynn, R.B., Blackbourn, G. and Gibson, O. (2007b) Evolution of turbidity currents deduced from extensive thin turbidites: Marnoso Arenacea Formation (Miocene), Italian Apennines. *Journal of Sedimentary Research*, **77**, 172-196.172-196

Talling, P.J., Wynn, R.B., Masson, D.G., Frenz, M., Cronin, B.T., Schiebel, R., Akhmetzhanov, A.M., Dallmeier-Tiessen, S., Benetti, S., Weaver, P.P.E., Georgiopoulou, A., Zuhlsdorff, C. and Amy, L.A. (2007c) Onset of submarine debris flow deposition far from original giant landslide. *Nature*, **450**, 541-544.541-544

Talling, P.J., Malgesini, G., Sumner, E.J., Amy L.A., Felletti, F., Blackbourn, G., Nutt, C., Wilcox, C., Harding, I.C., and Akbari, S. (2012b) Planform geometry, stacking pattern, and extra-basinal origin of low-strength and higher-strength cohesive debris flow deposits in

the Marnoso-arenacea Formation. Geosphere. doi:
10.1130/GES00734.1

Talling, P.J., Sumner, E.J., Masson, D.G., and Malgesini, G. (2012a) Subaqueous sediment density flows: depositional processes and deposit types. *Sedimentology*, 10.1111/j.1365-3091.2012.01353.x

Torfs, H., Mitchener, H., Huysentruyt, H. and Toorman, E. (1996) Settling and consolidation of mud/sand mixtures. *Coastal Engineering*, **27-45**, 27-45.27-45

Trowbridge, J.H. and Kineke, G.C. (1994) Structure and dynamics of fluid muds on the Amazon Continental-Shelf. *Journal of Geophysical Research-Oceans*, **99**, 865-874.865-874

Vrolijk, P.J. and Southard, J.B. (1997) Experiments on rapid deposition of sand from high-velocity flows. *Geoscience Canada*, **24**, 45-54.45-54

Walker, R.G. (1967) Turbidite sedimentary structures and their relationship to proximal and distal environments. *Journal of Sedimentary Petrology*, **37**, 24-43.24-43

Weaver, P.P.E. (1991) Quaternary high-resolution stratigraphy and its application in studies of the Canary Basin. *Aapg Bulletin-American Association of Petroleum Geologists*, **75**, 1424-1424.1424-1424

Weaver, P.P.E. (1994) Determination of turbidity current erosional characteristics from reworked coccolith assemblages, Canary Basin northeast Atlantic. *Sedimentology*, **41**, 1025-1038.1025-1038

Weaver, P.P.E. and Kuijpers, A. (1983) Climatic control of turbidite deposition on the Madeira Abyssal Plain. *Nature*, **306**, 360-363.360-363

Weaver, P.P.E. and Rothwell, R.G. (1987) Sedimentation on the Madeira Abyssal Plain over the last 300,000 years. . In: *Weaver, P.P.E., Thomson, J. (Eds.), Geology and Geochemistry of Abyssal Plains. Geol. Soc. Spec. Publ. No. 31, pp. 71-86.*, **31**, 71-86.71-86

Weaver, P.P.E., Rothwell, R.G., Ebbing, J., Gunn, D. and Hunter, P.M. (1992) Correlation, frequency of emplacement and source directions of megaturbidites on the Madeira Abyssal Plain. *Marine Geology*, **109**, 1-20.1-20

Weaver, P.P.E. and Thomson, J. (1993) Calculating erosion by deep-sea turbidity currents during initiation and flow. *Nature*, **364**, 136-138.136-138

Whitehouse, R., Soulsby, R., Roberts, W. and Mitchener, H. (2000) Dynamics of Estuarine Muds. . *HR Wallingford and Thomas Telford, London*, 210.210

Winterwerp, J.C. and van Kesteren, W.G.M. (2004) Introduction to the physics of cohesive sediment in the marine environment. *Developments in Sedimentology*, **56**, Elsevier

Wood, A. and Smith, A.J. (1958) The sedimentation and sedimentary history of the Aberystwyth Grits (Upper Llandoveryan). *Quarterly Journal of the Geological Society*, **114**, 163-195.163-195

Wright, L.D., Friedrichs, C.T., Kim, S.C. and Scully, M.E. (2001) Effects of ambient currents and waves on gravity-driven sediment transport on continental shelves. *Marine Geology*, **175**, 25-45.25-45

Wynn, R.B., Talling, P.J., Masson, D.G., Le Bas, T.P., Cronin, B.T. and Stevenson, C.J. (2012) The influence of subtle gradient changes on deep-water gravity flows: a case study from the Moroccan Turbidite system. *Application of the principles of seismic geomorphology to continental-slope and base-of-slope systems: Case studies from seafloor and near seafloor analogues*, **SEPM Special Publication 99**, 371-383.371-383

Wynn, R.B., Talling, P.J., Masson, D.G., Stevenson, C.J., Cronin, B.T. and Le Bas, T.P. (2010) Investigating the Timing, Processes and Deposits of One of the World's Largest Submarine Gravity Flows: The 'Bed 5 Event' Off Northwest Africa. In: *Submarine Mass Movements and Their Consequences* (Eds D.C. Mosher, R.C. Shipp, L. Moscardelli, J.D. Chaytor, C.D.P. Baxter, H.J. Lee and R. Urgeles), *Advances in Natural and Technological Hazards Research*, **28**, pp. 463-474. Springer, Dordrecht.

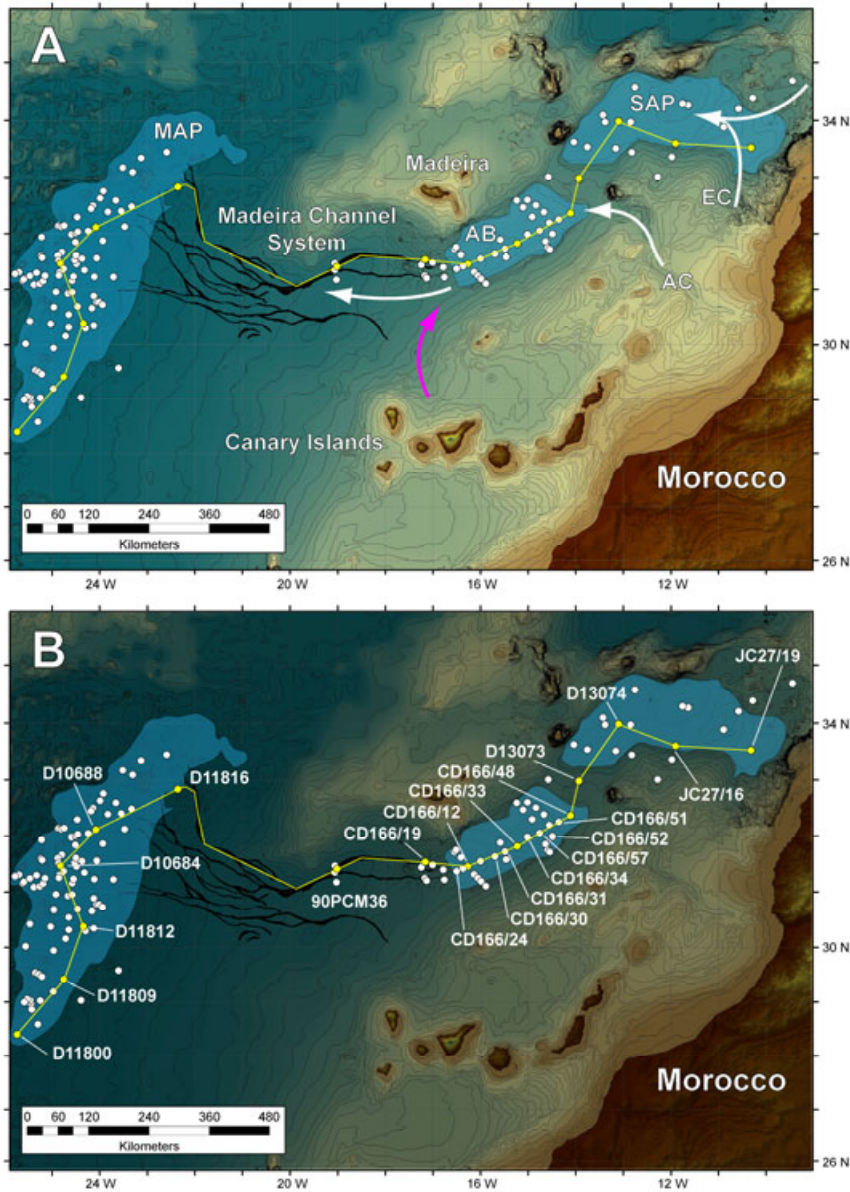
Wynn, R.B., Weaver, P.P.E., Masson, D.G. and Stow, D.A.V. (2002) Turbidite depositional architecture across three interconnected deep-water basins on the north-west African margin. *Sedimentology*, **49**, 669-695.669-695

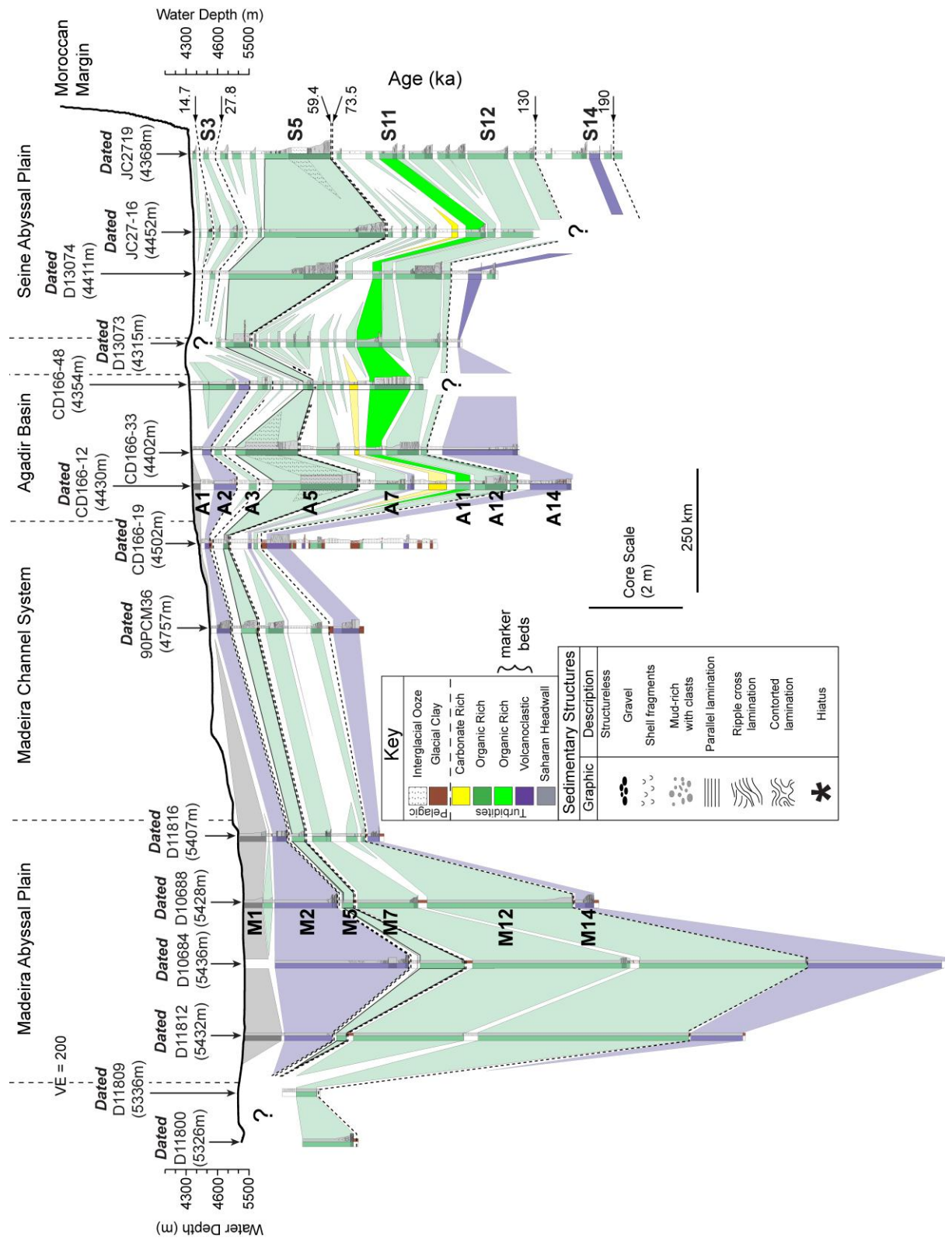
Bed	Position in deposit*	Number observed	Grading below break	Grading above break	Grain size below break	Grain size above break	Facies below break	Facies above break
<i>Type I – Gravel overlain by finer sand</i>								
5	Lower Proximal	11	Normal, Ungraded	Ungraded Normal Inverse	650 – >1000	300 – 650	ST (Gravel)	ST
12	Lower Proximal	1**	Ungraded	Inverse	400	200	ST	ST
<i>Type II – Inversely graded sand overlain by finer sand</i>								
5	Lower Proximal	2	Inverse	Normal	> 1000	600	ST	PL
12	Lower Proximal	1**	Inverse	Normal	700	300	ST	PL
<i>Type III – Sand overlain by finer sand</i>								
11	Lower Middle	5	Normal	Normal	90 – 100	60 – 70	PL	CL
<i>Type IV – sand overlain by mud</i>								
3	Upper Proximal Central Distal	13	Normal	Ungraded Normal	100 – 200	10 – 30	ST	M
5	Upper Proximal Central Distal	34	Normal	Ungraded Normal	90 – 210	10 – 30	ST PL	M CM L
7	Upper Proximal Central Distal	22	Normal	Ungraded Normal	90 – 100	10 – 25	RXL	M CM L
11	Upper Proximal Central Distal	18	Normal	Ungraded Normal	90 – 180	10 – 30	PL CL	M CM L
12	Upper Proximal Central Distal	34	Normal	Ungraded Normal	70 – 90	7 – 20	PL CL ST	M CM L
<i>Type V – Mud-rich sand overlain by mud</i>								
5	Upper Distal	5	Ungraded Normal	Ungraded	100 – 210	20 – 30	ST _D	M CM

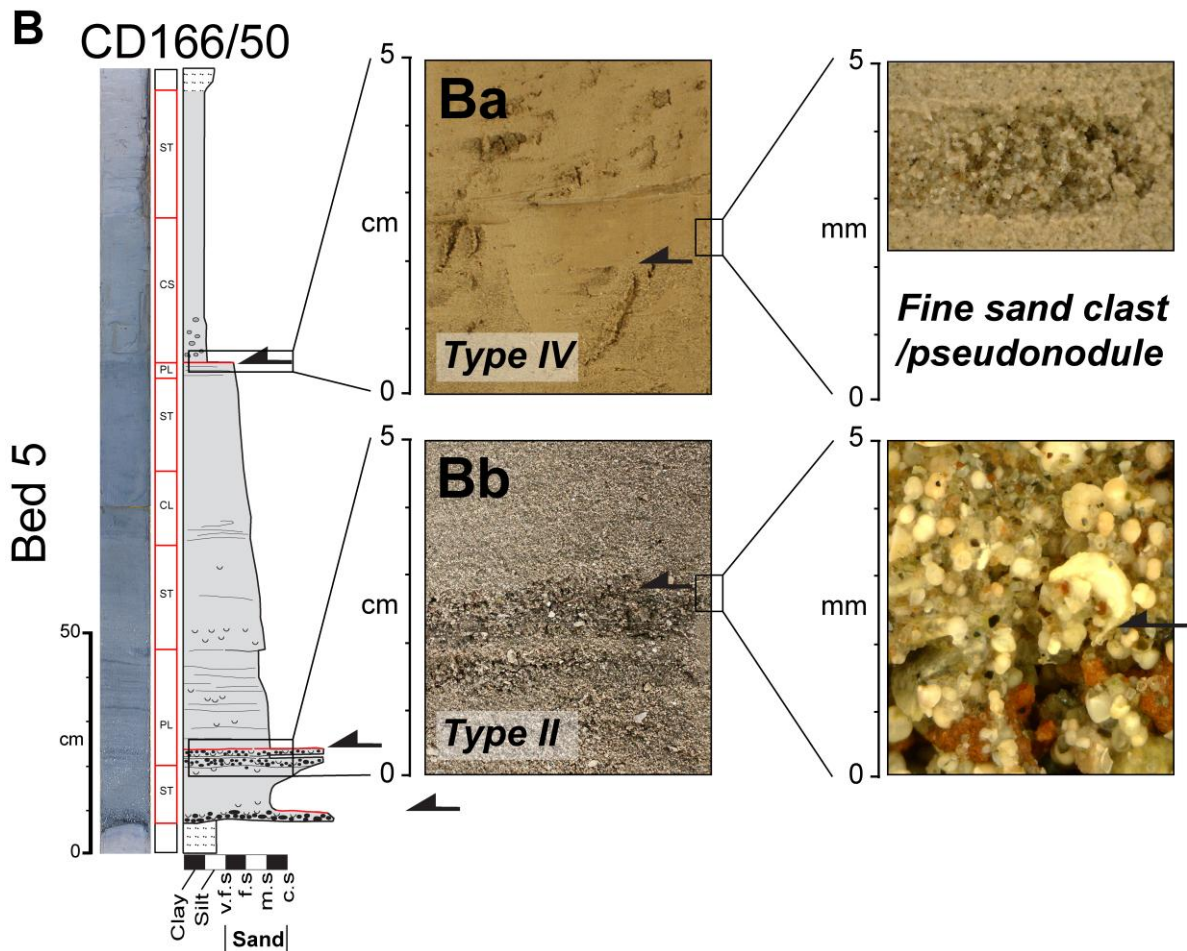
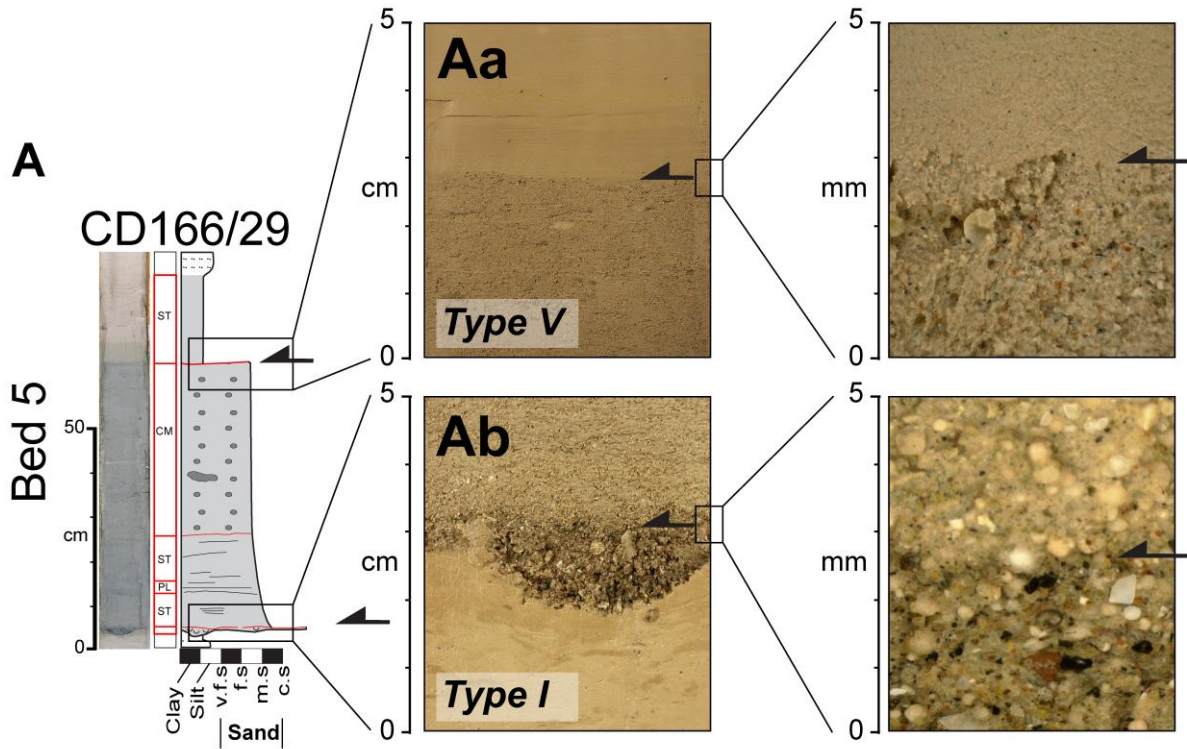
Table 1. Summarizing the five different types of grain size break found within the Moroccan Turbidite System, in Beds 3, 5, 7, 11 and 12.

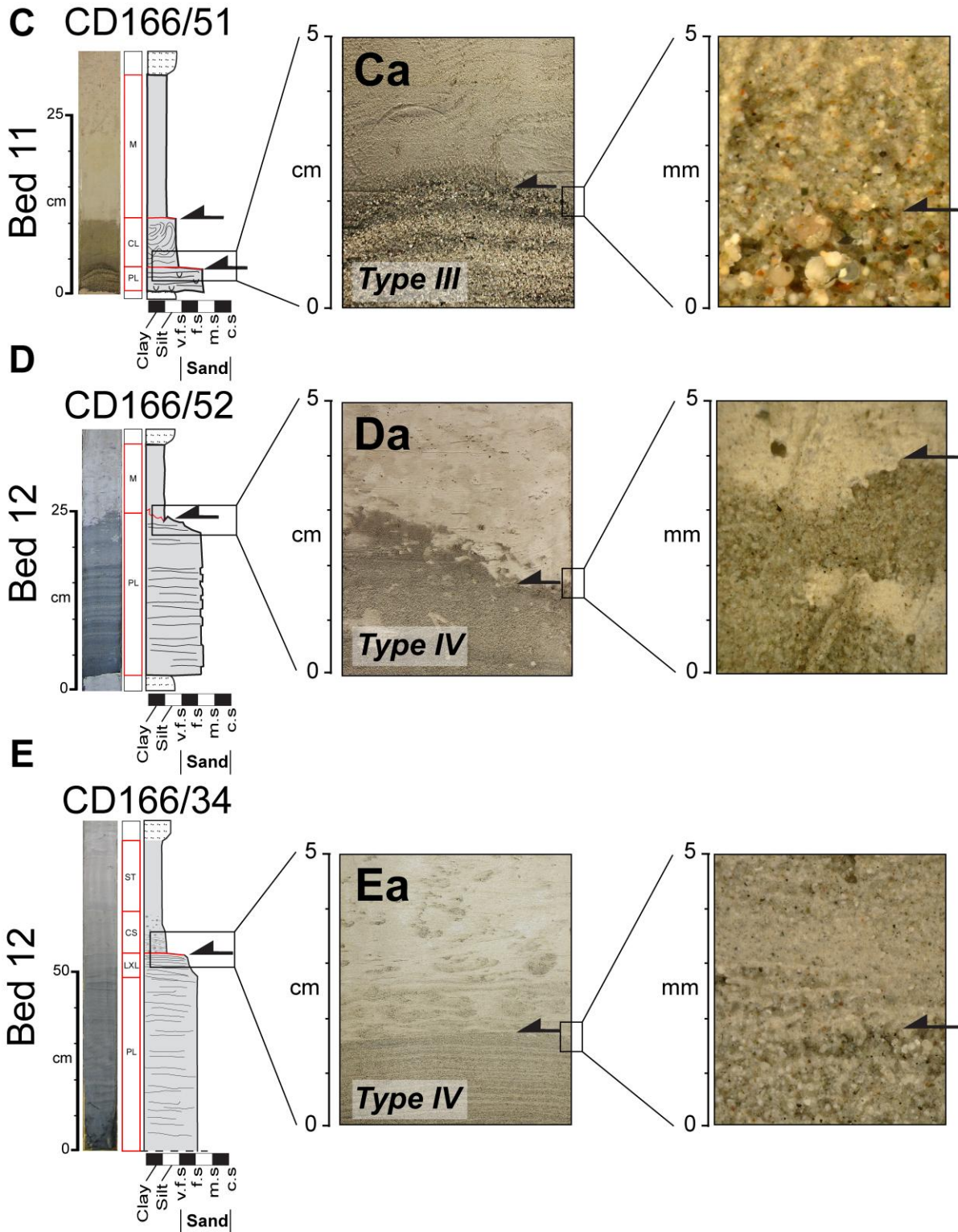
* Lower, middle and upper refer to the vertical position within the deposits. Proximal, central and distal refer to the distance deposits are located from source.

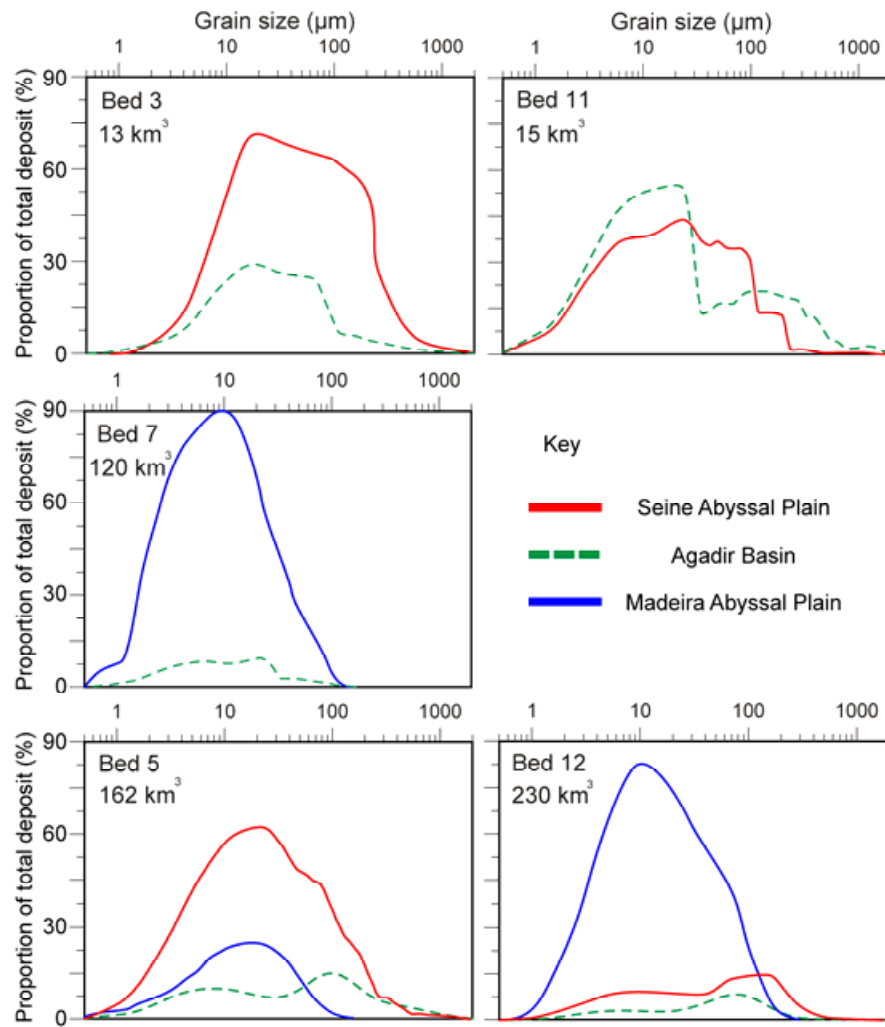
** A number of cores do not fully penetrate the proximal deposit

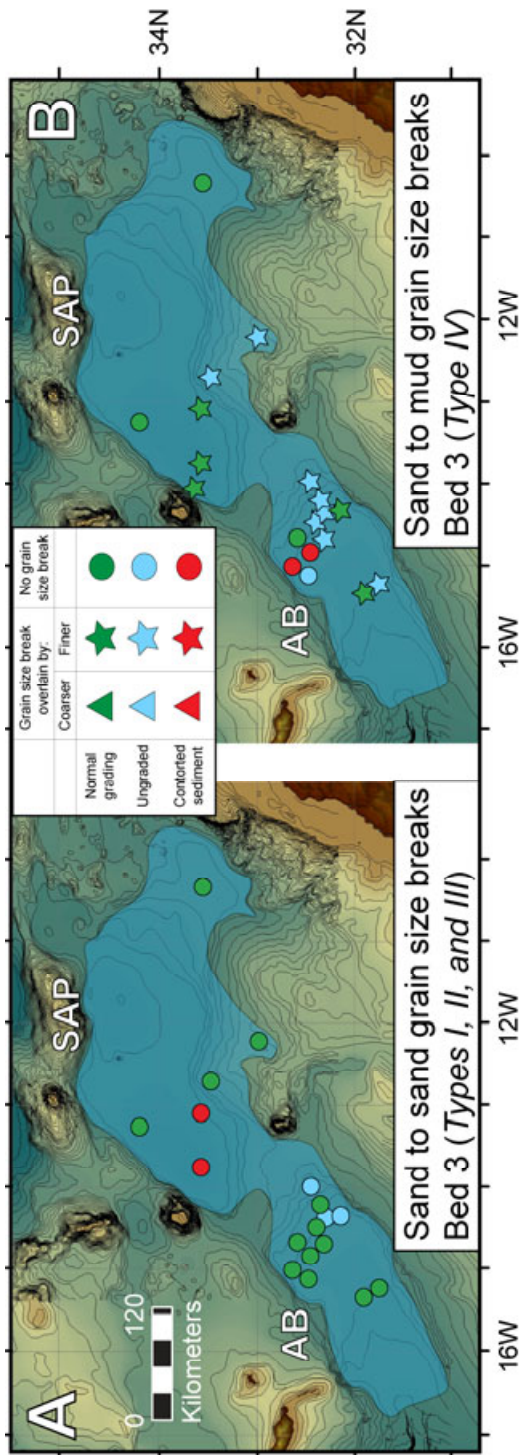


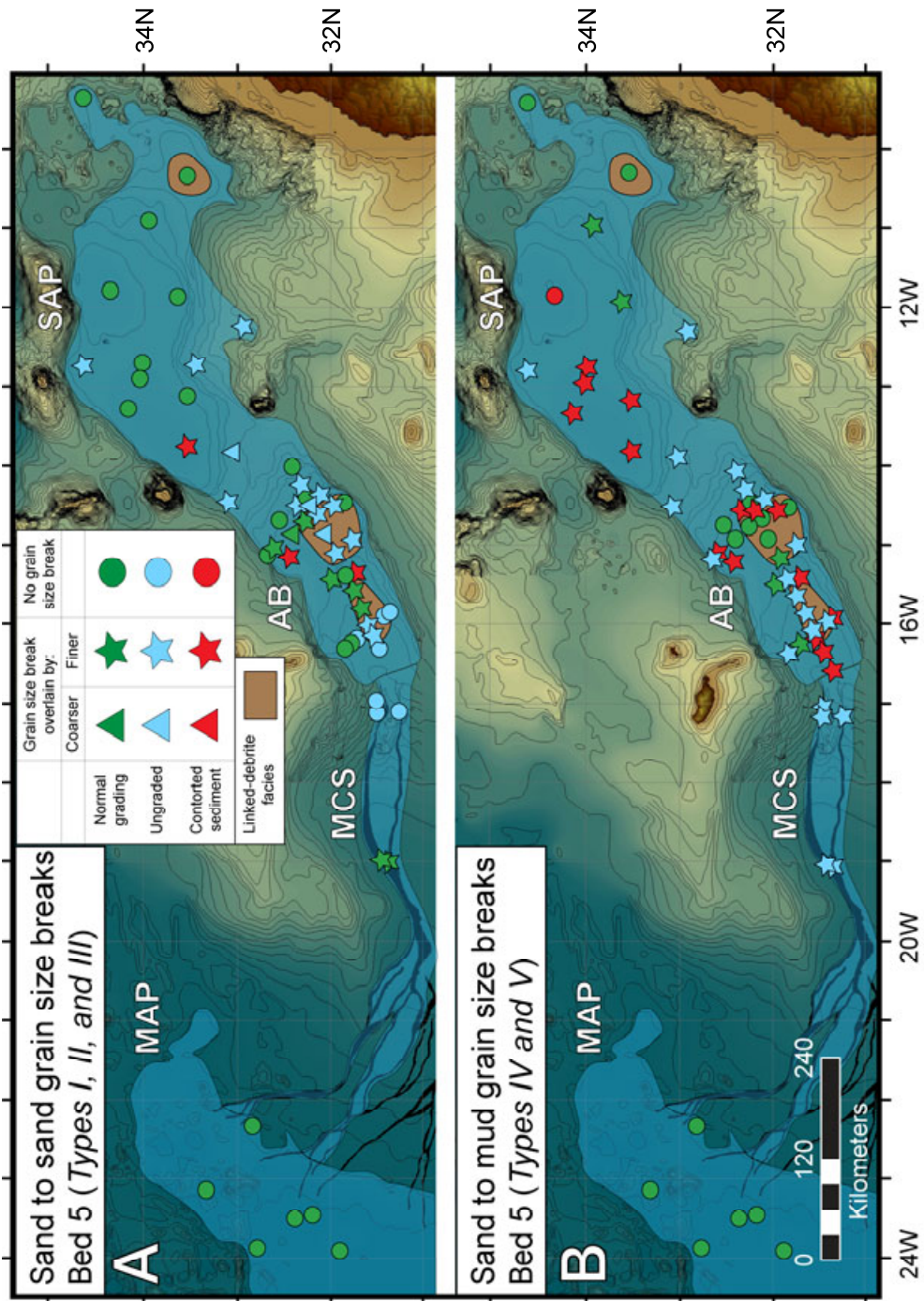


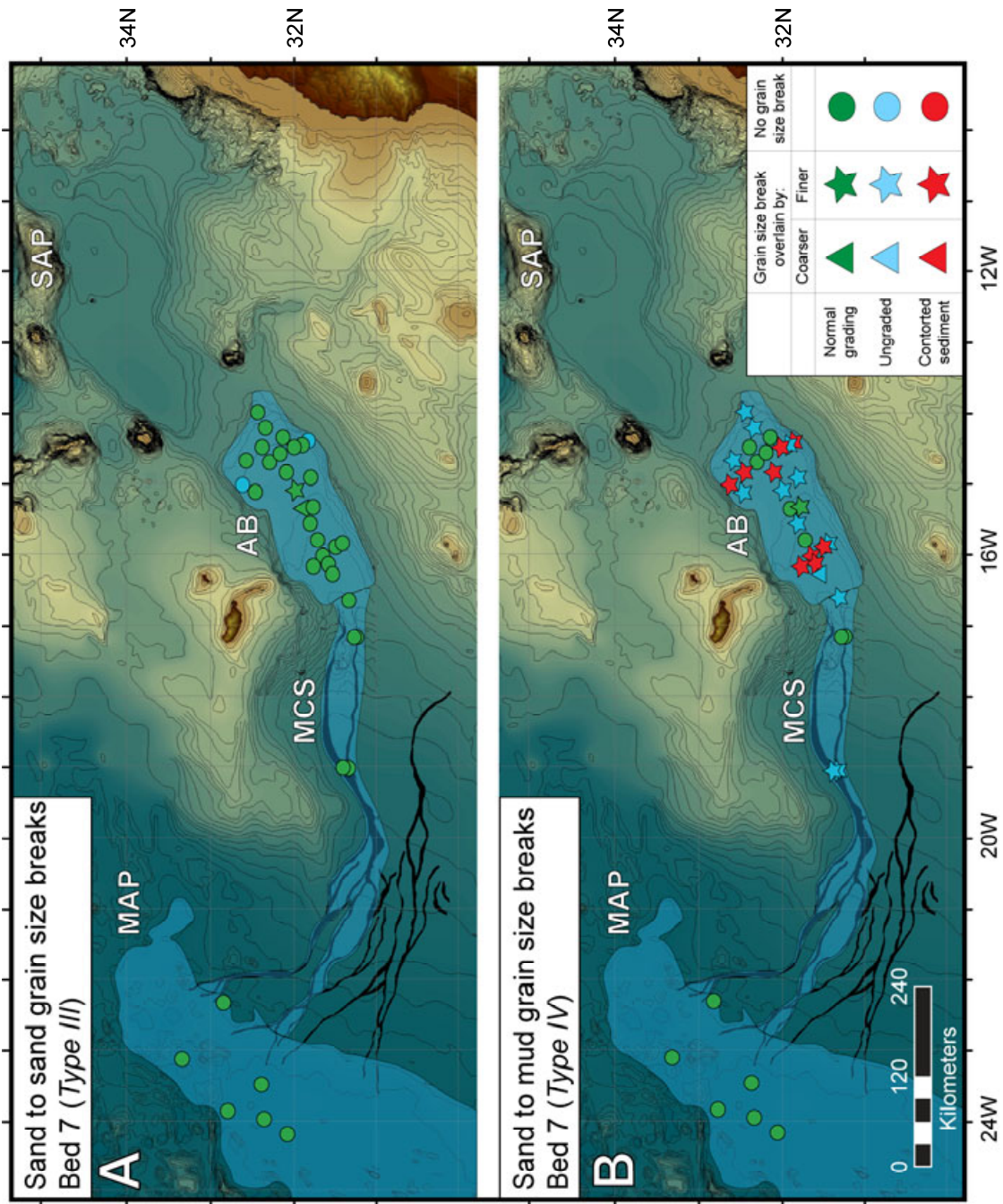


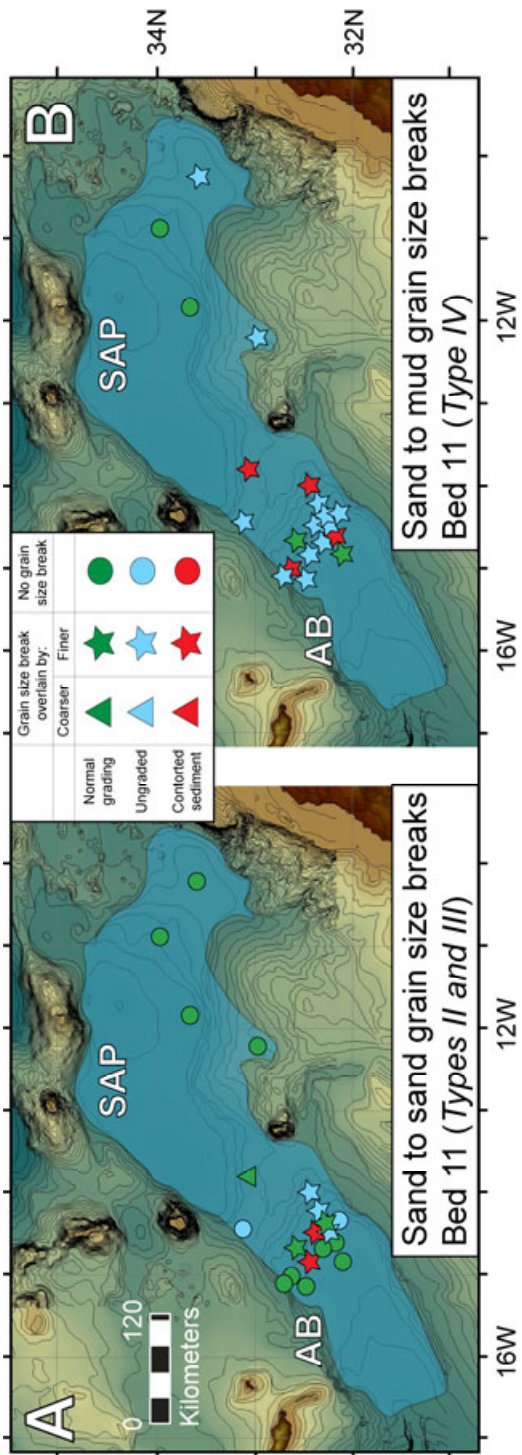


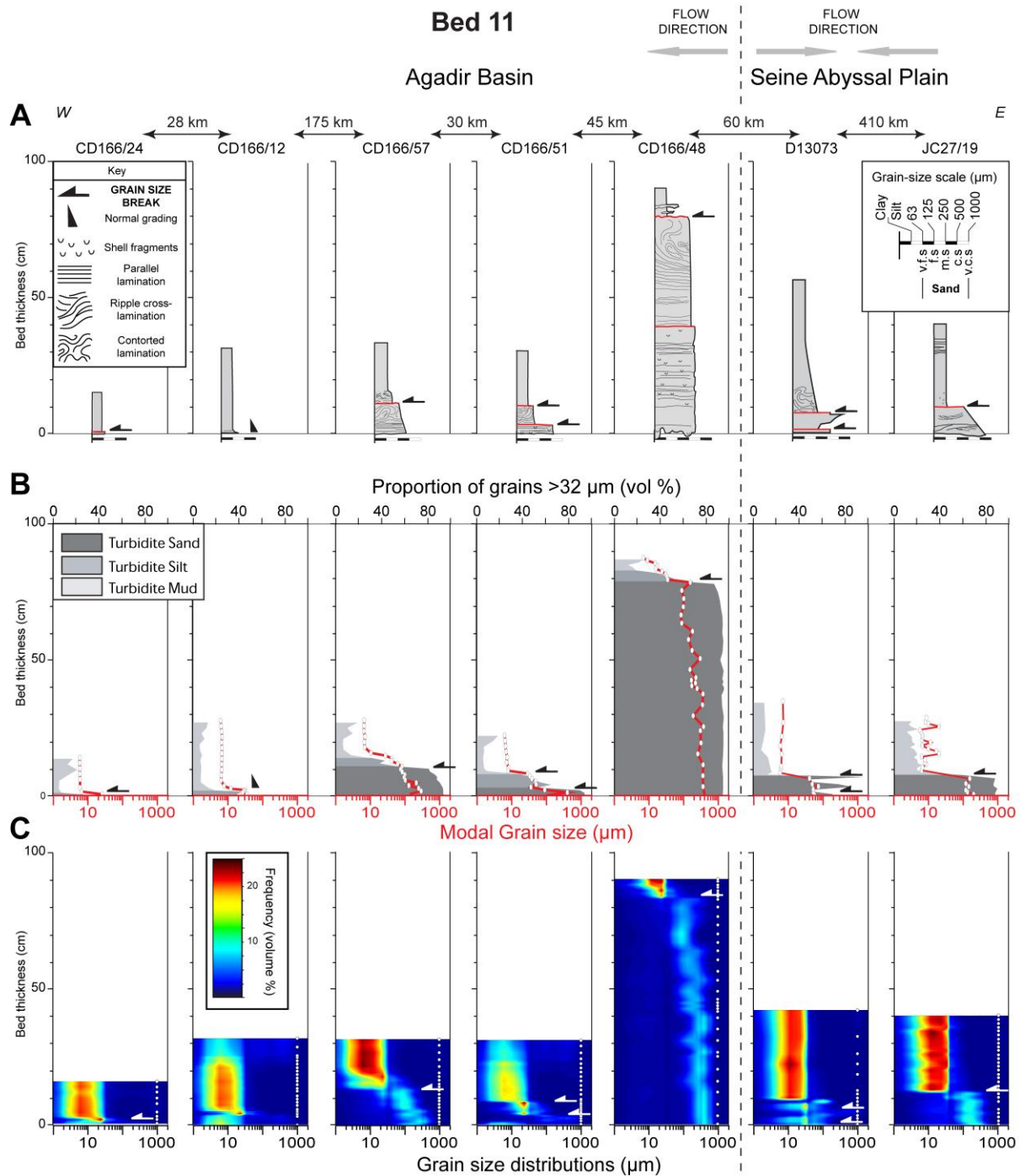


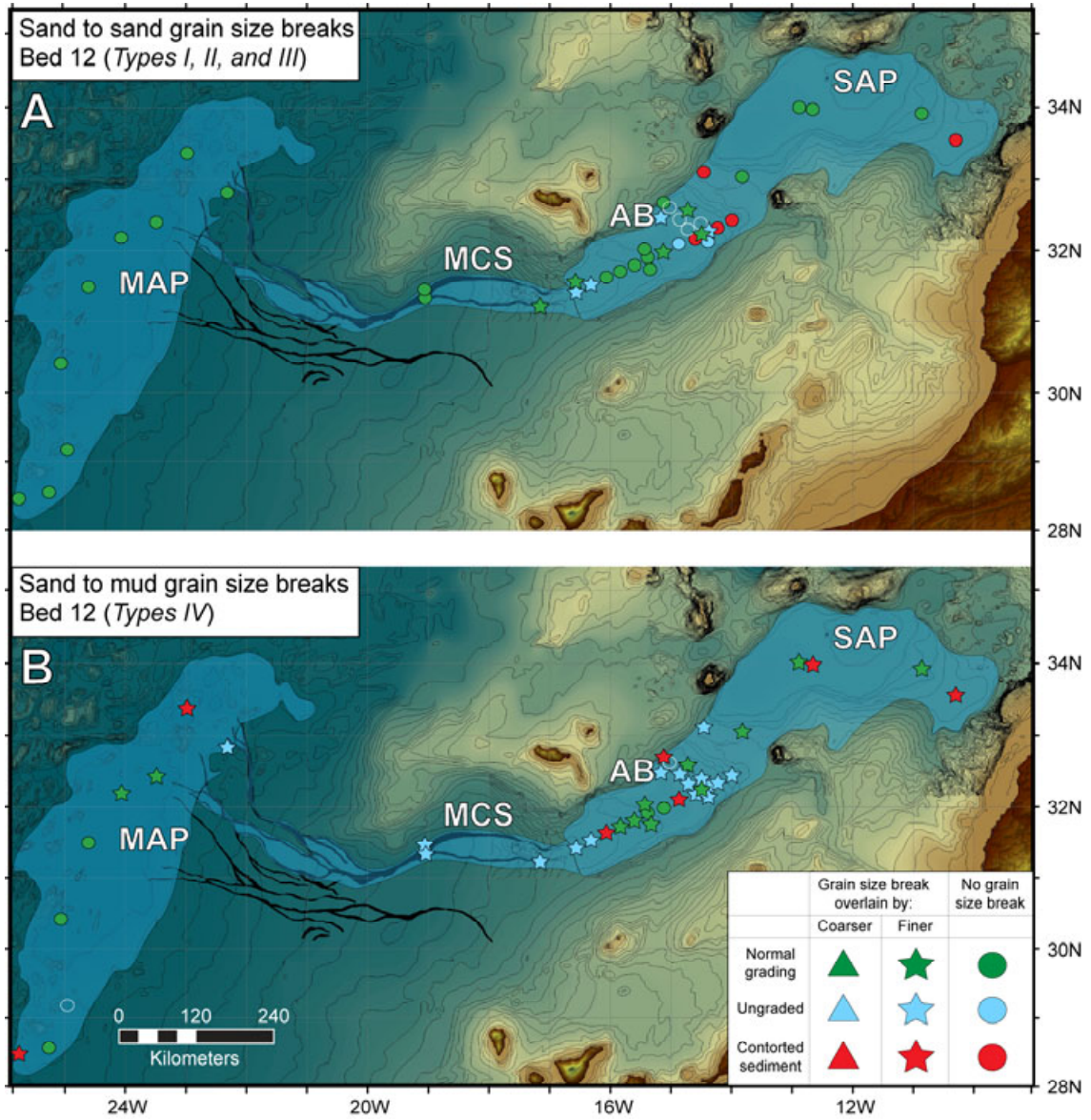


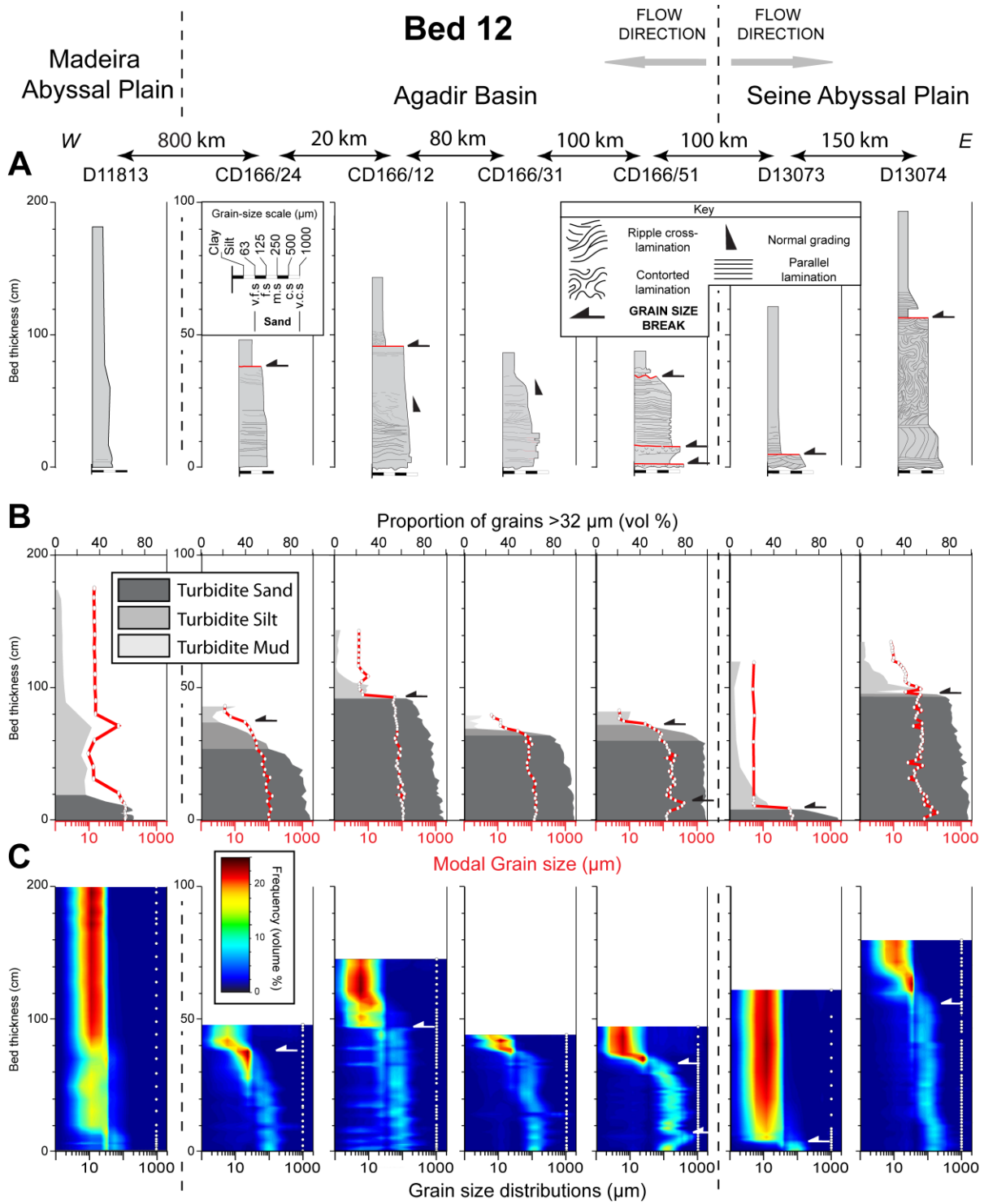




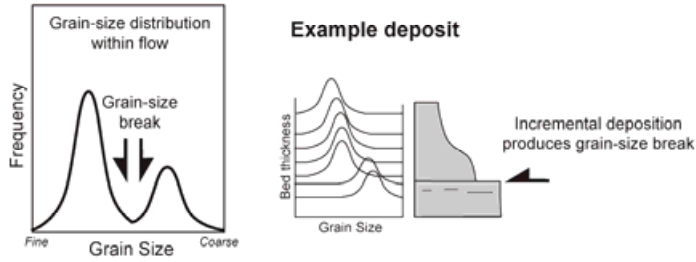




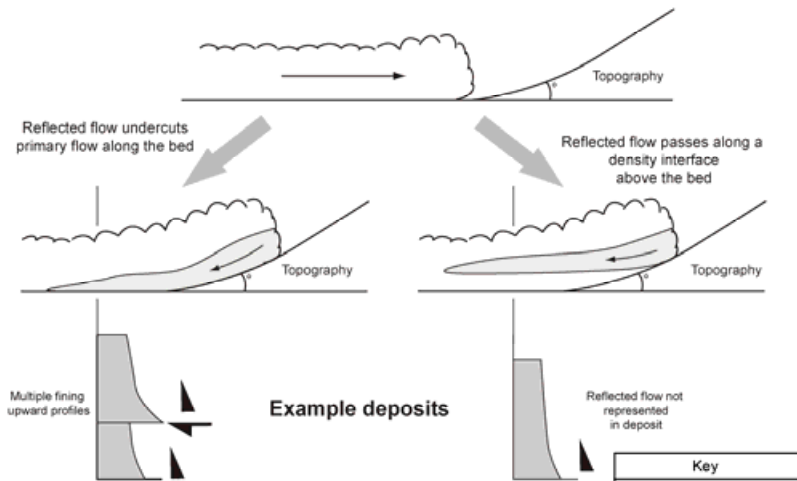




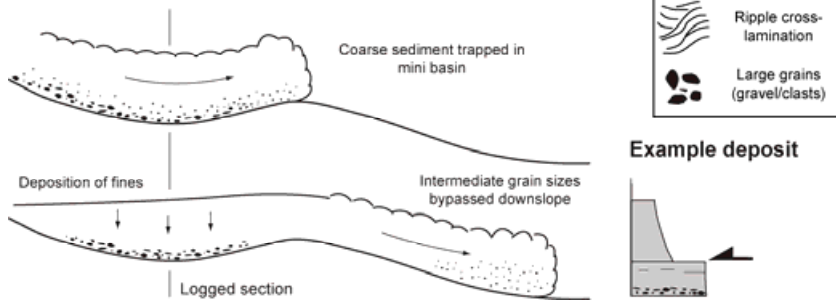
A) Bimodal grain-size distribution within flow



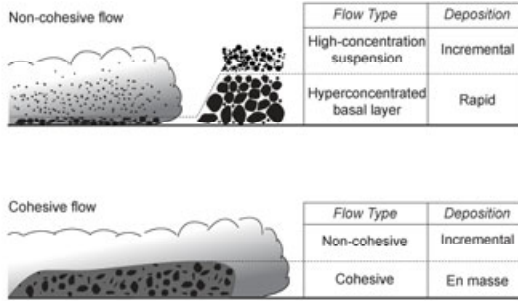
B) Flow Reflection



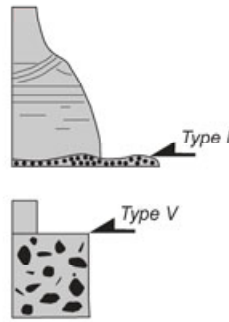
C) Flow Separation



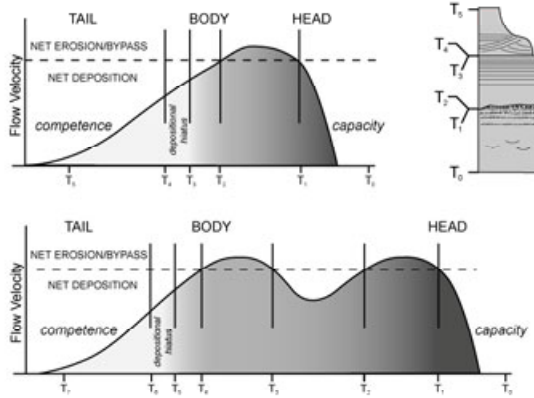
A) Vertical flow stratification



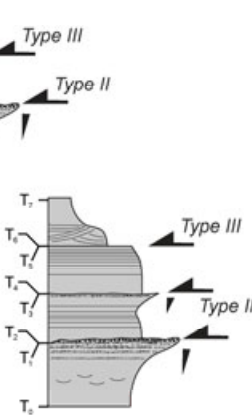
Example deposits



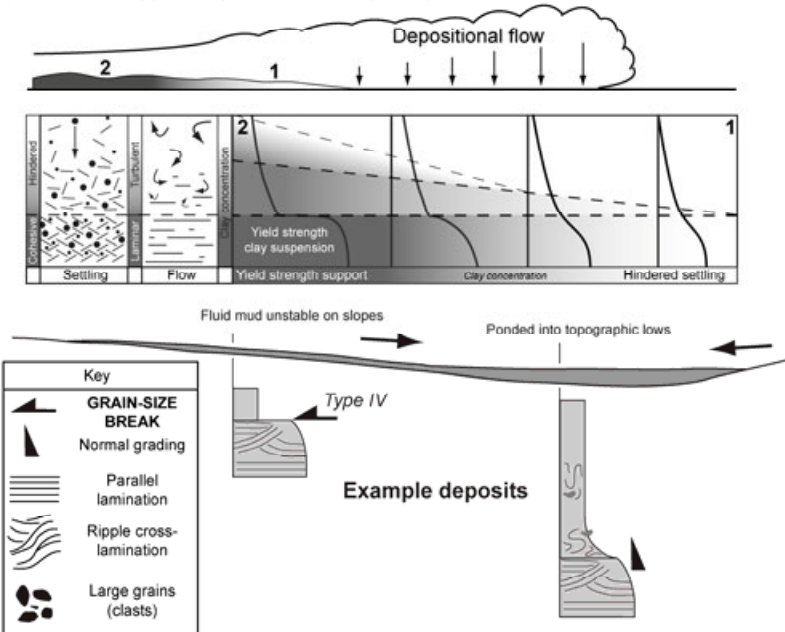
B) Fluctuations in flow capacity

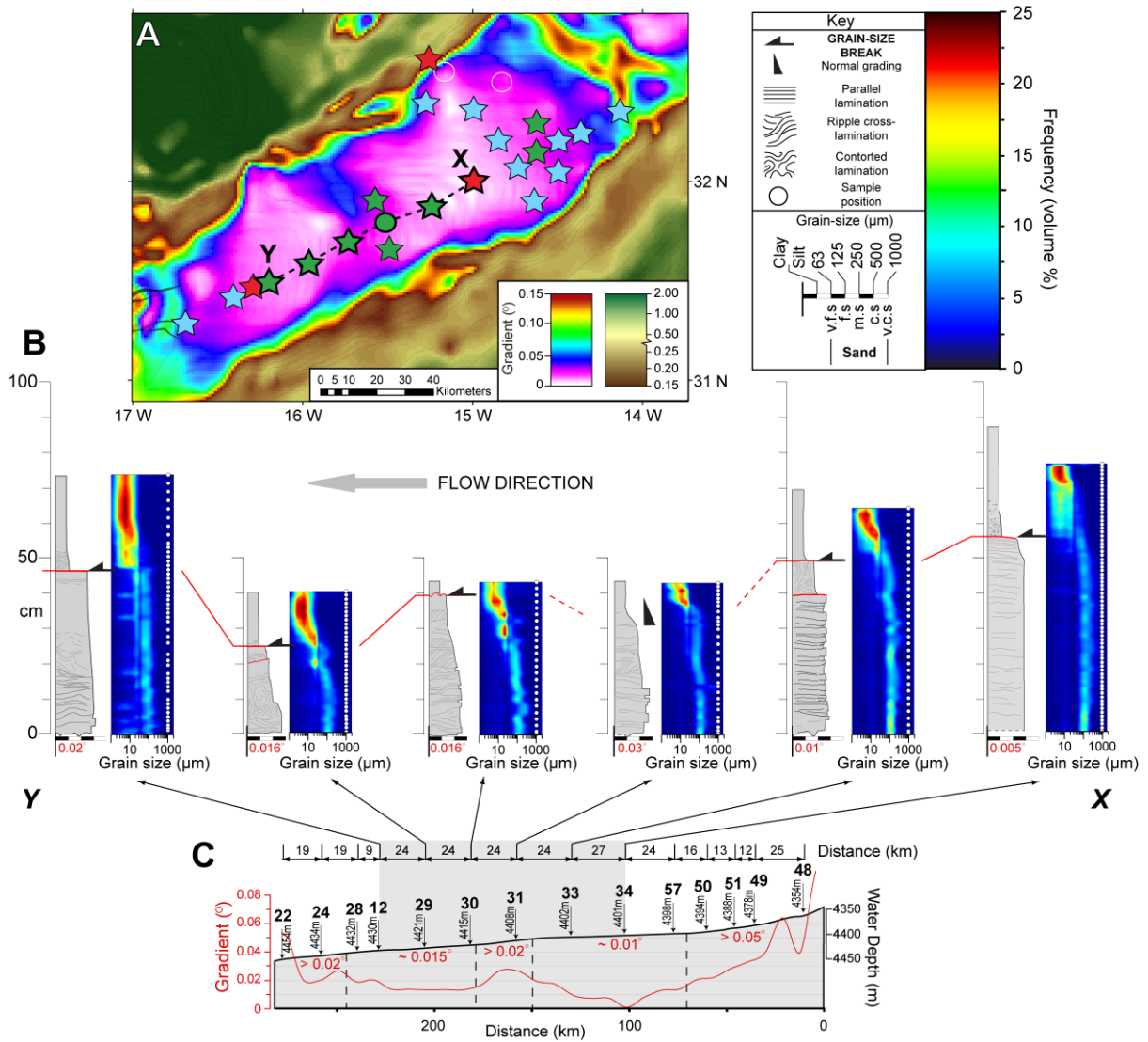


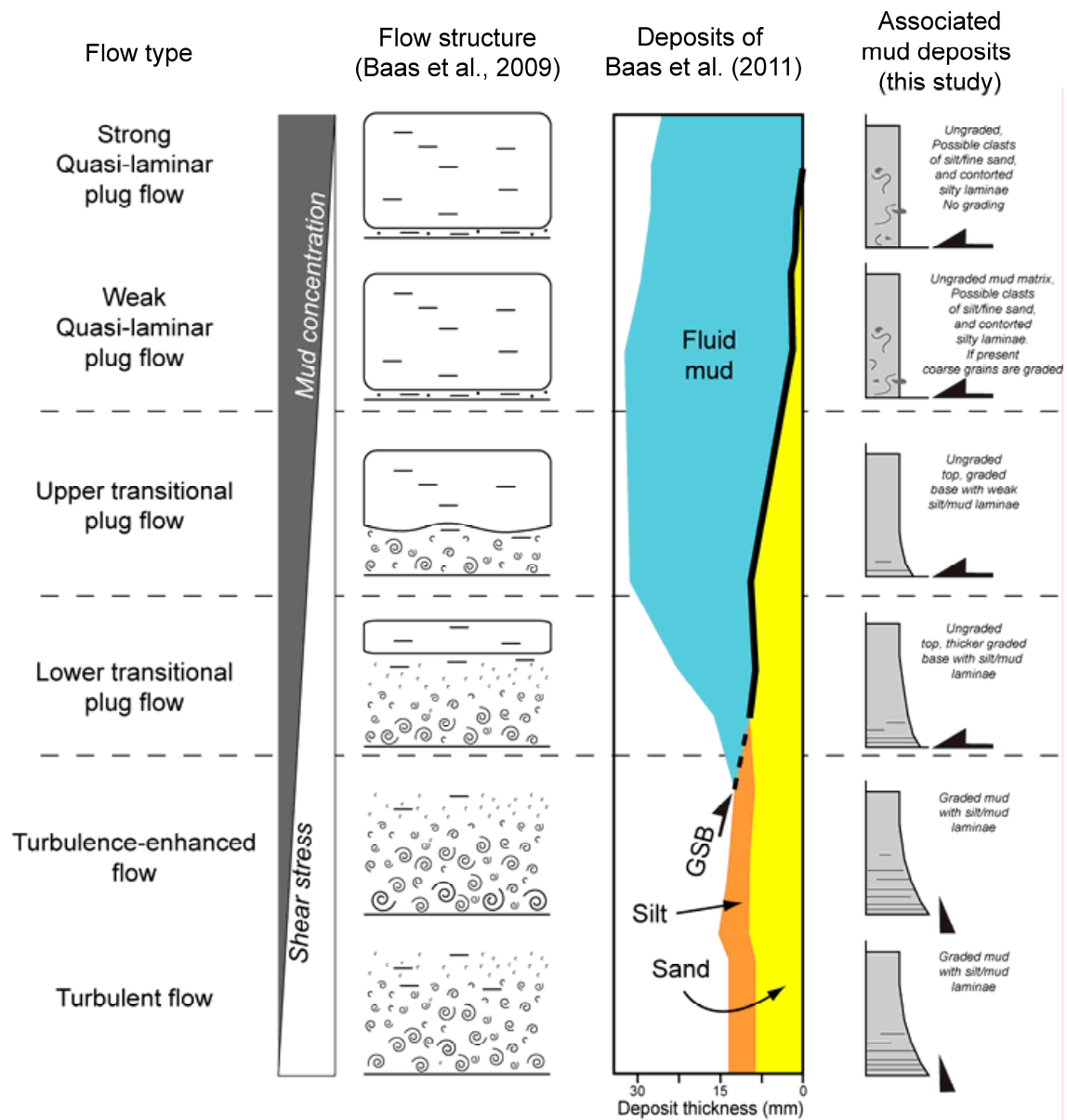
Example deposits



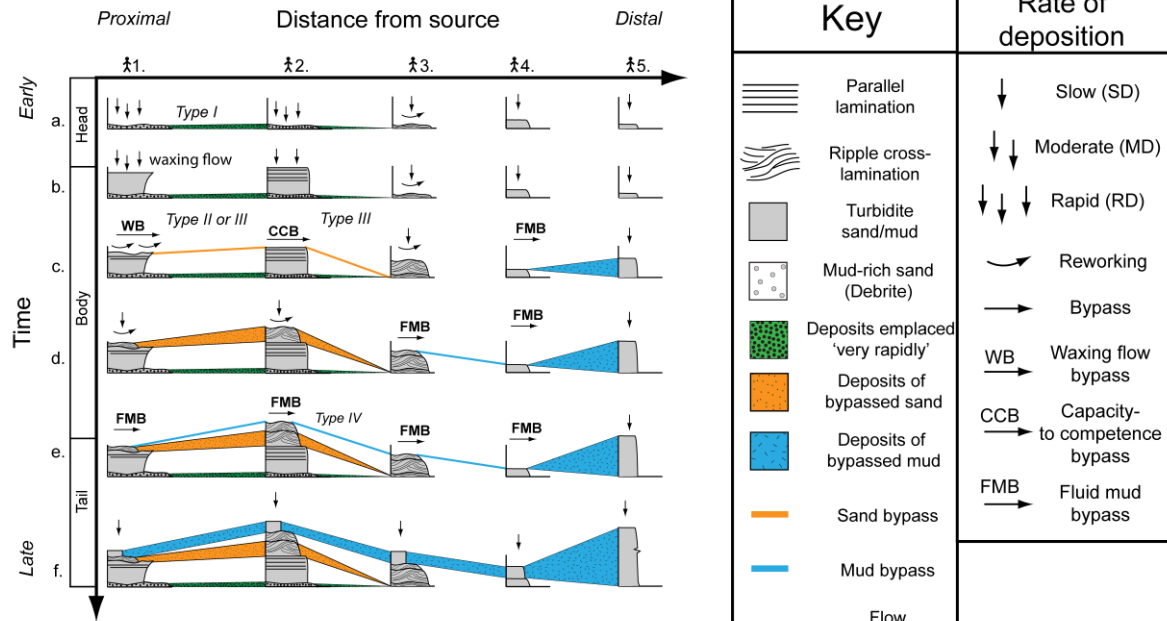
C) Sediment bypass by cohesive clay suspensions







A. Deposits



B. Flow Processes

